Statistical mechanics of one-dimensional Ginzburg-Landau fields. II. A test of the screening approximation (n^{-1} expansion)

Richard A. Ferrell*

Center for Theoretical Physics, University of Maryland, College Park, Maryland 20742

Douglas J. Scalapino†

Department of Physics, University of California, Santa Barbara, California 93105
(Received 24 September 1973)

The free-energy density of a one-dimensional Ginzburg-Landau field with n components ϕ_i is identified with the quantum-mechanical ground-state energy of an n-dimensional anharmonic oscillator. Normalizing the anharmonic term by $(4n)^{-1}$ and expanding in powers of n^{-1}, we find for the ground-state energy, $n E_\infty + E^{(1)} + n^{-1} E^{(2)}$, where $E_\infty = \kappa/2 - 1/16\kappa^2$, and $E^{(1)} = (\kappa_2 - 2\kappa)/2$ and $E^{(2)} = 3\kappa_2^{-2} - 6\kappa \; \kappa_2^{-3} - (11/4)\kappa^{-1} \; \kappa_2^{-4}$ are the Hartree and first and second screening approximations, respectively. κ and $\kappa_2 = (4\kappa^2 + \kappa^{-1})^{1/2}$ are the inverse correlation lengths for ϕ_i and $\Sigma \phi_i^2$, respectively. The temperature is linearly related to the spring constant τ, which in turn is connected with the correlation lengths by $\tau = \kappa^2 - 1/2\kappa$. The analytic results are compared with exact numerical computations for $n = 1, 2, 3,$ and 4. The second screening correction modestly improves the accuracy of the approximation.

I. INTRODUCTION

The phenomenon of a phase transition of second order is encountered in systems of various spatial dimensionality D and order-parameter dimensionality n. Although $D = 3$ is the case most commonly observed in the laboratory, $D = 2$ and even $D = 1$ are not without experimental interest. On the theoretical side, the pioneering solution of Onsager[1] for $D = 2$ and $n = 1$ (Ising model) is the cornerstone of the entire subject. It is therefore useful to attempt to solve the statistical-mechanics problem posed by phase transitions for various choices of D in the Ginzburg-Landau model. For $D = 1$, the one-dimensional problem is especially rewarding as it lends itself to exact solution. Unfortunately, the sharp transition which occurs for $D \geq 2$ disappears for $D = 1$,[2,3] but this does not prevent one from calculating in detail some physically measurable quantity, such as the specific heat, as a function of temperature. This has, in fact, been carried out and published for both $n = 1$ and $n = 2$.[4-7] Furthermore, as we shall see below, there are additional numerical results contained in these references which indirectly specify the thermodynamic functions for $n = 3$ and $n = 4$.

The purpose of the present paper is to study the systematic trend exhibited by the exact solutions referred to above. It is well known that a general solution to the phase-transition problem, the so-called "screening solution," can be obtained for $n \gg 1$ as a Taylor-series expansion in powers of n^{-1}.[8,9] To any finite order, and especially in referring to the first correction of $O(n^{-1})$, we call

this method the "screening approximation." Thus our goal here is to compare the trend exhibited by the exact solutions, as n increases, with the screening approximation. As we shall see, although the comparison can only be expected to become exact for very large values of n, it is in fact surprisingly good even for relatively small n.

After a review of basic preliminaries we discuss in Sec. II the simplification of the problem which results from a kind of stochastic peaking which sets in as $n \to \infty$. In Sec. III we review the extreme case $n = \infty$, the so-called "Hartree limit." This is followed in Sec. IV by a review of the Feynman sum over paths which converts the task of calculating the transfer matrix into the familiar problem of solving the Schrödinger equation.[10] In this formulation the thermodynamic free energy becomes the quantum-mechanical ground-state-energy eigenvalue. In Sec. V we do the quantum mechanics to $O(n^{-1})$ to find the first correction to the Hartree approximation. This permits a comparison of the screening approximation with the exact solutions for the free energy, the entropy, and the specific heat. Section VI is devoted to $O(n^{-2})$. In Sec. VII we present some results from perturbation theory and establish that the screening approximation in its more familiar field-theoretic form is equivalent to the n^{-1} correction calculated in Sec. V. Section VIII concludes with a brief summary.

Although the most familiar one-dimensional phase transition is perhaps that of a superconductor ($n = 2$), for the sake of simplicity we begin our discussion of statistical mechanics with

$n = 1$. We imagine that the system is described by the real order parameter $\overline{\phi}(x)$ at any point x along the filament and that the free-energy density at that point, in units of the Boltzmann constant times the temperature, is given by the Ginzburg–Landau functional[11]

$$F = \tfrac{1}{2}Z^{-1}\left(\frac{\partial\overline{\phi}}{\partial x}\right)^2 + \tfrac{1}{2}a\overline{\phi}^2 + \tfrac{1}{4}b\overline{\phi}^4 \ . \qquad (1.1)$$

Because of the unidimensionality, the coefficients a and b have dimensions of linear density times $[\overline{\phi}]^{-2}$ and $[\overline{\phi}]^{-4}$, respectively. $[\overline{\phi}]$ denotes the dimensions of $\overline{\phi}$. Similarly Z^{-1} has dimensions of length times $[\overline{\phi}]^{-2}$. Thus we are led to form characteristic parameters from these coefficients. For the moment we avoid a, which depends linearly on the temperature and changes sign in the critical region, and we use only b and Z^{-1}. The latter are taken to be temperature-independent constants in the model. As $\overline{\phi}$ is simply a variable of integration in the functional integration which we will need to carry out, any physically significant parameter should be independent of $[\overline{\phi}]$. This feature is exhibited by the combination bZ^2, which has the dimensions of (length)$^{-3}$. Consequently we define a characteristic length ξ_c by

$$\xi_c^{-3} = bZ^2 \ . \qquad (1.2)$$

(For general spatial dimensionality, we have to write ξ_c^{-4+D} on the left-hand side.[12]) Using this characteristic length we can reduce all remaining lengths to dimensionless form. In particular, we replace the distance coordinate x by the dimensionless variable u according to

$$x = \xi_c u \ . \qquad (1.3)$$

Now the free-energy density per unit distance measured in terms of u is given by

$$\xi_c F = \tfrac{1}{2}Z^{-1}\xi_c^{-1}\left(\frac{\partial\overline{\phi}}{\partial u}\right)^2 + \tfrac{1}{2}a\xi_c\,\overline{\phi}^2 + \tfrac{1}{4}b\xi_c\,\overline{\phi}^4 \ . \qquad (1.4)$$

This expression can be simplified by changing the normalization of the order-parameter field $\overline{\phi}$ and introducing a new field ϕ according to

$$\overline{\phi}^2 = Z\xi_c\,\phi^2 \ . \qquad (1.5)$$

Defining the reduced relative temperature τ as

$$\tau = \xi_c^2 Za \qquad (1.6)$$

and substituting for $\overline{\phi}$ in terms of ϕ in Eq. (1.4) gives now the free-energy density in the standard form[12]

$$\xi_c F = -L = \frac{1}{2}\left(\frac{\partial\phi}{\partial u}\right)^2 + \frac{\tau}{2}\,\phi^2 + \tfrac{1}{4}\phi^4 \ . \qquad (1.7)$$

Here we have denoted the dimensionless quantity

$\xi_c F$ as the negative of an effective "Lagrangian" L. In terms of L, the partition function for a system of length Ω is given by the functional integral

$$Z_\Omega = \int \delta\phi \exp\left(\int_\Omega L\,du\right) \ . \qquad (1.8)$$

The thermodynamic free-energy density (again in units of the Boltzmann constant times temperature) is

$$\mathfrak{F} = -(1/\Omega)\ln Z_\Omega \ . \qquad (1.9)$$

All of the above is readily generalized to an n-component order parameter ϕ_i $(i = 1,\ 2,\ \ldots,n)$ interacting via an isotropic quartic term. The Lagrangian is then

$$L_n = -\frac{1}{2}\sum_{i=1}^{n}\left[\left(\frac{\partial\phi_i}{\partial u}\right)^2 + \phi_i^2\left(\tau + \frac{1}{2n}\sum_{j=1}^{n}\phi_j^2\right)\right], \qquad (1.10)$$

with the thermodynamic free-energy density per degree of freedom (i.e., per component)

$$\mathfrak{F}_n = -(1/n\Omega)\ln Z_\Omega^{(n)} \ . \qquad (1.11)$$

(Here, as before, we are measuring energy in units of the Boltzmann constant times temperature.) $Z_\Omega^{(n)}$ is the obvious generalization of Eq. (1.8), with L_n in place of L. Figure 1 exhibits the results of the numerical calculations of $\mathfrak{F}_n$
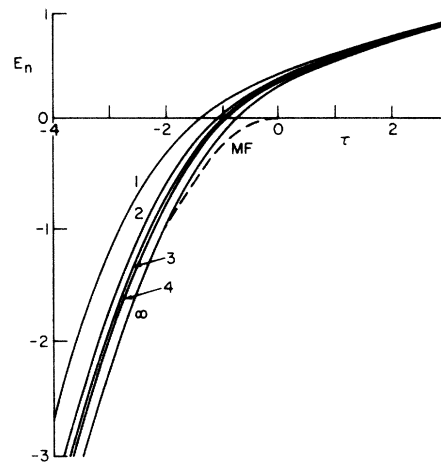

FIG. 1. Ground-state energy divided by n, E_n, vs spring constant τ of an isotropic n-dimensional anharmonic oscillator. The coefficient of the anharmonic term is normalized to $(4n)^{-1}$. E_n is also the thermodynamic free-energy density per degree of freedom of an n-component isotropic Ginzburg–Landau field in one dimension, in which case τ is the reduced temperature. The cases $n = 1$, 2, 3, 4, and ∞ ("Hartree limit") are shown by the solid curves. The dashed curve (MF) illustrates the mean-field approximation.

(labeled E_n in the figure) for $n = 1$, 2, 3, and 4, which will be discussed in further detail below in Sec. IV. The Hartree limit derived below in Sec. III is shown by the curve labeled ∞, and the mean-field (MF) approximation by the dashed curve. Weakening the interaction as $n \to \infty$ by including the factor n^{-1} in the last term of Eq. (1.10) is essential for obtaining the Hartree limit, as will become evident in Sec. III [see especially Eq. (3.1)].

For some purposes it is more convenient to deal with the entropy rather than the free energy. This is found by calculating the negative first derivative of the free energy with respect to the temperature parameter τ. We prefer to deal with a function which is -2 times this quantity, which we shall nevertheless call the "entropy function," and which is given by

$$\theta_n = 2 \frac{\partial \mathfrak{F}_n}{\partial \tau} . \tag{1.12}$$

These functions for $n = 1$, 2, 3, and 4 are shown by the curves in Fig. 2, where the mean-field approximation now appears as the dashed straight line. By a kind of Ward's identity which follows from differentiating inside the functional integral, we obtain

$$\theta_n = \langle \phi_i^2 \rangle = (1/n) \langle \phi^2 \rangle , \tag{1.13}$$

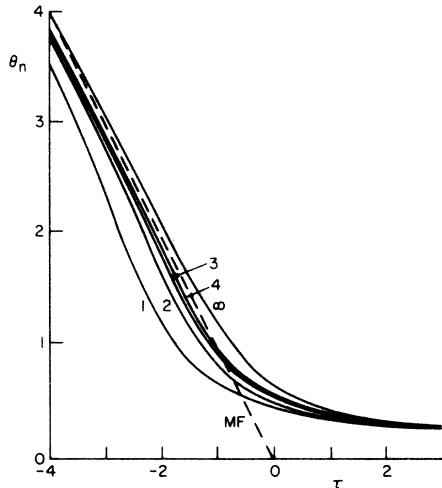where ϕ_i is one of the n components of the field and ϕ^2 is the sum of all of the squares,

$$\phi^2 \equiv \sum_{i=1}^{n} \phi_i^2 . \tag{1.14}$$

The angular brackets denote the thermal-equilibrium average defined by the functional integral

$$\langle A \rangle = Z_\Omega^{-1} \int \prod_i \delta \phi_i A \exp\left(\int_\Omega L_n \, du \right) . \tag{1.15}$$

Differentiating the entropy function, we obtain the specific heat

$$C_n = \frac{\partial \theta_n}{\partial \tau} = -2 \frac{\partial^2 \mathfrak{F}_n}{\partial \tau^2} , \tag{1.16}$$

normalized to unity in the limit $\tau \to -\infty$. The numerical results for C_n are shown by the curves $n = 1$, 2, 3, and 4 in Fig. 3, with the mean-field approximation represented by the step function. It will be noted that these curves and those of Figs. 1 and 2 exhibit a definite regularity as a function of the parameter n. In Secs. II and III we will study some simplifying features which set in in the limit $n \to \infty$.

II. STOCHASTIC PEAKING

In this section we want to demonstrate a simplification which enters the statistical-mechanics problem posed in Sec. I when the number of components becomes very large ($n \gg 1$). We will demonstrate this in a particularly simple limiting situation, $\tau \gg 1$, for which we can neglect the interaction between the components of the fluctuating field. First we Fourier analyze the order parameter according to
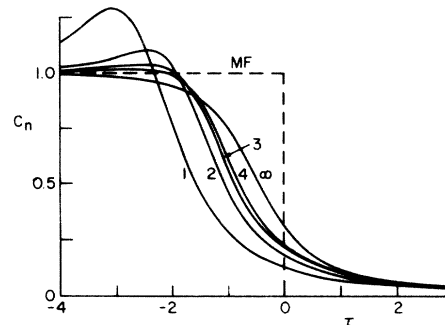
$$\phi = \Omega^{-1/2} \sum_q \phi_q e^{iqu} . \tag{2.1}$$

FIG. 2. Entropy function $\theta_n = 2 \partial E_n / \partial \tau$ vs reduced temperature τ. The cases $n = 1$, 2, 3, 4, and ∞ are shown by the solid curves. (θ_∞ is alternatively denoted by θ in the text.) The mean-field approximation is illustrated by the dashed line (MF). The thermodynamic entropy density of an n-component isotropic Ginzburg–Landau field in one dimension is proportional to $-\theta_n$.

FIG. 3. Specific heat $C_n = -2 \partial^2 E_n / \partial \tau^2$ vs reduced temperature τ. C_n is normalized to unity in the limit $\tau \to -\infty$. The cases $n = 1$, 2, 3, 4, and ∞ are shown by the solid curves, and the dashed line (MF) illustrates the mean-field approximation. A sum rule requires that the area under each of the solid curves be independent of n and equal to the area under the dashed line.

For the moment we work with a single-component field. The integral over the Lagrangian in terms of the Fourier components ϕ_q is

$$\int_\Omega L \, d\Omega = -\tfrac{1}{2} \sum_q (q^2 + \tau) |\phi_q|^2, \qquad (2.2)$$

where the interaction has been dropped. Substituting Eq. (2.2) into Eq. (1.8) replaces the functional integral by the multiple integral over the Fourier components,

$$Z_\Omega = \int \prod_q d^2\phi_q \, e^{-(q^2+\tau)|\phi_q|^2/2}$$

$$= \prod_q \left(\frac{\pi}{q^2+\tau}\right)^{1/2}. \qquad (2.3)$$

The free energy, according to Eq. (1.9), is given by

$$\mathcal{F} = \frac{-1}{\Omega} \ln Z_\Omega$$

$$= \frac{1}{2\Omega} \sum_q \ln(q^2 + \tau) + C$$

$$= \frac{1}{4\pi} \int_{-q_D}^{q_D} dq \, \ln(q^2 + \tau) + C, \qquad (2.4)$$

where C is a constant and where the sum over wave numbers has been replaced by an integral extending between the Debye cutoffs at $\pm q_D$. Carrying out this integral yields the following dependence on the temperature variable τ and the Debye cutoff q_D:

$$\int_0^{q_D} dq \, \ln(q^2 + \tau) = 2\tau^{1/2} \tan^{-1}(q_D/\tau^{1/2})$$

$$+ q_D \ln(q_D^2 + \tau) - 2q_D$$

$$\simeq \pi\tau^{1/2} - \tau/q_D + 2q_D(\ln q_D - 1). \qquad (2.5)$$

The last line is valid for $q_D \gg 1$. This gives us a dependence on τ which in the limit $q_D \to \infty$ is expressed solely by the first term, the last term being absorbed by a redefinition of the zero of energy according to

$$\mathcal{F} = E + C'. \qquad (2.6)$$

Here we have separated off the constant addition to the energy and described what is left by the energy function

$$E(\tau) = \tfrac{1}{2}\tau^{1/2}. \qquad (2.7)$$

The entropy function is found from Eq. (1.12) to be

$$\theta(\tau) = 1/2\tau^{1/2}. \qquad (2.8)$$

This result could alternatively be obtained directly from Eq. (2.4) by differentiating inside the integral before carrying out the integration. Alternatively, it can be obtained from the expression for the mean-square fluctuation in the Fourier component of the order parameter,

$$\langle |\phi_q|^2 \rangle = 1/(q^2 + \tau). \qquad (2.9)$$

According to Eq. (1.13) the entropy function can be regarded as the sum of the mean-square fluctuations in the Fourier components of the order parameter field,

$$\theta = \langle \phi^2 \rangle = \Omega^{-1} \sum_q \langle |\phi_q|^2 \rangle$$

$$\simeq \frac{1}{2\pi} \int_{-q_D}^{q_D} \frac{dq}{q^2 + \tau} \simeq \frac{1}{2\tau^{1/2}}, \qquad (2.10)$$

in complete agreement with Eq. (2.8).

The above result enables us to write the probability distribution for the ith component of the multicomponent order parameter as the Gaussian function

$$P_i(\phi_i) = (2^{-1}\theta_n^{-1}/\pi)^{1/2} e^{-\phi_i^2/2\theta_n}$$

$$= (\tau^{1/4}/\sqrt{\pi}) e^{-\tau^{1/2}\phi_i^2}, \qquad (2.11)$$

where the variance of the field is $\theta_n = \theta$ and is given by Eq. (2.10). We are dealing with a multicomponent field and therefore have to consider the over-all probability distribution function for the totality of all n components, which is expressed by the product

$$\prod_{i=1}^{n} P_i(\phi_i) = (\tau^{n/4}/\pi^{n/2}) e^{-\tau^{1/2}\phi^2}. \qquad (2.12)$$

At this point we note that the distribution depends upon the field only through the sum $\phi^2 = \sum \phi_i^2$ and does not depend upon the components ϕ_i individually. Consequently, we change to hyperspherical coordinates and make use of ϕ as a "radial" coordinate. Because of the lack of dependence upon direction, we integrate over all solid angles, which brings in the area of the n-dimensional unit hypersphere

$$C_n = \frac{2\pi^{n/2}}{\Gamma(n/2)}. \qquad (2.13)$$

Thus the radial probability distribution is

$$P(\phi) \, d\phi = C_n \phi^{n-1} \, d\phi \prod_i P_i(\phi_i), \qquad (2.14)$$

where

$$P(\phi) = \frac{2\tau^{n/4}}{\Gamma(n/2)} e^{-M(\phi)} \qquad (2.15)$$

and

$$M(\phi) = \tau^{1/2} \phi^2 - (n-1)\ln\phi . \qquad (2.16)$$

The minimum of this function, corresponding to the peak in the probability distribution, is found from

$$M'(\phi_{min}) = 2\tau^{1/2}\phi_{min} - (n-1)/\phi_{min} = 0 \qquad (2.17)$$

or

$$\phi_{min}^2 = (n-1)/2\tau^{1/2} . \qquad (2.18)$$

We will need the curvature and the third derivative at the minimum. These are given by

$$M''(\phi_{min}) = 2\tau^{1/2} + (n-1)/\phi_{min}^2 = 4\tau^{1/2} \qquad (2.19)$$

and

$$M'''(\phi_{min}) = -2(n-1)/\phi_{min}^3 . \qquad (2.20)$$

The Taylor-series expansion for $M(\phi)$ to third order in $\phi - \phi_{min}$ is

$$M(\phi) \simeq \tau^{1/2}\phi_{min}^2 - (n-1)\ln\phi_{min} + \tfrac{1}{2}M''(\phi_{min})(\phi - \phi_{min})^2$$
$$+ \tfrac{1}{6}M'''(\phi_{min})(\phi - \phi_{min})^3$$
$$= \frac{n-1}{2} - \frac{n-1}{2}\ln\frac{n-1}{2} + (n-1)\ln\tau^{1/4}$$
$$+ 2\tau^{1/2}(\phi - \phi_{min})^2 - \frac{1}{3}\frac{n-1}{\phi_{min}^3}(\phi - \phi_{min})^3 .$$
$$(2.21)$$

For the moment we do not need the cubic term and indicate it simply by the word "cubic." The first two terms can be recognized as related for large values of $(n-1)/2$ to the Γ function, by Stirling's formula. Consequently we have

$$M(\phi) \simeq -\ln\frac{\Gamma((n+1)/2)}{[\pi(n-1)]^{1/2}} + (n-1)\ln\tau^{1/4}$$
$$+ 2\tau^{1/2}(\phi - \phi_{min})^2 + \text{cubic} . \qquad (2.22)$$

We also note that asymptotically

$$\frac{\Gamma((n+1)/2)}{\Gamma(n/2)} \sim (n/2)^{1/2} . \qquad (2.23)$$

Substituting these expressions into Eq. (2.15) and simplifying gives

$$P(\phi) \simeq (2\tau^{1/2}/\pi)^{1/2} e^{-2\tau^{1/2}(\phi - \phi_{min})^2 + \text{cubic}} , \qquad (2.24)$$

a Gaussian distribution centered at ϕ_{min} with variance equal to

$$\langle (\phi - \phi_{min})^2 \rangle = 1/4\tau^{1/2} . \qquad (2.25)$$

At this point we also can calculate the first

moment, which results from the small amount of skewness introduced by the cubic term. This can be calculated by expanding the exponential function of the cubic term in Eq. (2.24) in powers of the cubic term and keeping only the first power, leading to

$$\langle (\phi - \phi_{min}) \rangle \simeq \frac{n-1}{3\phi_{min}^3}\langle (\phi - \phi_{min})^4 \rangle$$
$$= \frac{n-1}{\phi_{min}^3}\langle (\phi - \phi_{min})^2 \rangle^2$$
$$= \frac{n-1}{16\tau\phi_{min}^3} = \frac{1}{8\tau^{1/2}\phi_{min}} . \qquad (2.26)$$

Replacing the fourth moment by three times the square of the second moment exploits a familiar property of the Gaussian distribution. We now obtain the entropy function from Eq. (1.13) by calculating the mean-square value of $\phi = (\phi - \phi_{min}) + \phi_{min}$. Substituting from Eqs. (2.18), (2.25), and (2.26) gives

$$n\theta_n = \langle \phi^2 \rangle = \phi_{min}^2 + \langle (\phi - \phi_{min})^2 \rangle + 2\phi_{min}\langle (\phi - \phi_{min}) \rangle$$
$$= \frac{n-1}{2\tau^{1/2}} + \frac{1}{4\tau^{1/2}} + \frac{1}{4\tau^{1/2}} = \frac{n}{2\tau^{1/2}} . \qquad (2.27)$$

Comparison of Eq. (2.27) with (2.8) shows $\theta_n = \theta$, as expected when the interaction between components can be neglected. The purpose of this exercise has been to exhibit the stochastic peaking which takes place for large values of n and which simplifies the statistical mechanics. As we shall see below, it is this simplification and the generation of the Gaussian distribution in the variable ϕ, even when interaction is present, which makes it possible to obtain results for all values of τ in the $n \gg 1$ regime.

III. HARTREE LIMIT

In this section we extend the idea of stochastic peaking, which was worked out in Sec. II for the case of no interaction, to the case where the fluctuations in the ϕ_i fields interact. The strength of the fluctuation in a particular component ϕ_i depends on the coefficient in Eq. (1.10) of $\phi_i^2/2$, which, in the absence of the quartic terms, is τ. Including the quartic terms gives an effective stiffness coefficient

$$\tau_{eff} = \tau + \frac{1}{n}\left(\sum_{j \neq i}\phi_j^2 + \tfrac{1}{2}\phi_i^2\right)$$
$$\simeq \tau + \frac{1}{n}\sum_{j=1}^{n}\phi_j^2 = \tau + \frac{1}{n}\phi^2$$
$$\simeq \tau + \theta_n . \qquad (3.1)$$

The second line follows from the addition of $\phi_i^2/2n$, a term of order n^{-1}. The third line results from neglecting the fluctuation in ϕ and replacing ϕ^2 by its mean value $n\theta_n$. From Eqs. (2.25) and (2.27) we see that this also entails an error of $O(n^{-1})$. As both approximations introduce errors of order $O(n^{-1})$, we see that Eq. (3.1) becomes accurate in the limit $n \to \infty$. In this limit, the "Hartree limit,"[13] we designate the entropy function θ_∞ simply by θ and obtain from Eq. (2.8) the self-consistency condition

$$\theta_\infty \equiv \theta = 1/2(\tau_{\text{eff}})^{1/2} = 1/2(\tau + \theta)^{1/2} \tag{3.2}$$

or

$$\tau = -\theta + 1/4\theta^2 . \tag{3.3}$$

Although we could eliminate θ from Eq. (3.3) by solving it as a cubic equation for θ in terms of τ, it is more convenient to keep θ as a parameter of the problem related to τ by Eq. (3.3). It is also convenient to introduce the inverse correlation length $\kappa = (\tau_{\text{eff}})^{1/2} = (2\theta)^{-1}$ and its noninteraction or "bare" value $\kappa_0 = \tau^{1/2}$. (The latter is defined only for positive τ.) In this notation Eq. (3.3) becomes

$$\tau = \kappa^2 - 1/2\kappa . \tag{3.4}$$

From Eq. (3.4) we have obtained the curve labeled "∞" in Fig. 2 of $\theta = (2\kappa)^{-1}$ vs τ. Equation (3.4) can be inverted for $\tau > 0$ to give the series expansion

$$\kappa = \kappa_0 + \tfrac{1}{4}\kappa_0^{-2} - \tfrac{3}{32}\kappa_0^{-5} + \tfrac{1}{16}\kappa_0^{-8} + \cdots$$

$$= \tau^{1/2} + \tfrac{1}{4}\tau^{-1} - \tfrac{3}{32}\tau^{-5/2} + \tfrac{1}{16}\tau^{-4} + \cdots . \tag{3.5a}$$

For negative τ we find the expansion

$$\kappa = \frac{1}{2|\tau|} - \frac{1}{8|\tau|^4} + \cdots . \tag{3.5b}$$

The general expression for the thermodynamic free-energy density per degree of freedom is readily obtained from Eq. (3.3) and from Ward's identity, Eq. (1.12):

$$E'_\infty(\tau) = \frac{\theta}{2} = \frac{\theta}{2} + \frac{1}{2}\frac{d\theta}{d\tau}\left(\tau + \theta - \frac{1}{4\theta^2}\right)$$

$$= \frac{d}{d\tau}\left(\frac{\tau}{2}\theta + \frac{1}{4}\theta^2 + \frac{1}{8\theta}\right) \tag{3.6}$$

The additional term, which vanishes by Eq. (3.3), enables us to write E'_∞ as a perfect derivative and to identify the Hartree energy as

$$E_\infty(\tau) = \frac{\tau}{2}\theta + \frac{1}{4}\theta^2 + \frac{1}{8\theta}$$

$$= -\frac{1}{4}\theta^2 + \frac{1}{4\theta} = \frac{\kappa}{2} - \frac{1}{16\kappa^2} . \tag{3.7}$$

In the second line, τ has been eliminated by means of Eq. (3.3). Equation (3.7) is illustrated by the curve labeled "∞" in Fig. 1. For the limiting case of very large positive τ we find from Eqs. (3.5a) and (3.7)

$$\theta(\tau \gg 1) = \tfrac{1}{2}\kappa^{-1} = \tfrac{1}{2}\kappa_0^{-1} - \tfrac{1}{8}\kappa_0^{-4} + \tfrac{5}{64}\kappa_0^{-7} + \cdots$$

$$= \frac{1}{2\tau^{1/2}} - \frac{1}{8\tau^2} + \frac{5}{64\tau^{7/2}} + \cdots , \tag{3.8}$$

$$E_\infty(\tau \gg 1) = \tfrac{1}{2}\kappa_0 + \tfrac{1}{16}\kappa_0^{-2} - \tfrac{1}{64}\kappa_0^{-5} + \cdots$$

$$= \frac{\tau^{1/2}}{2} + \frac{1}{16\tau} - \frac{1}{64\tau^{5/2}} + \cdots . \tag{3.9}$$

The first terms are simply Eqs. (2.8) and (2.7), and would give the entropy and energy accurately for all τ if there were no interaction. The second and third terms correspond to the interaction correction from first- and second-order perturbation theory, as demonstrated in Sec. VII. Note that each successive order of perturbation theory introduces a factor of $\kappa_0^{-3} = \tau^{-3/2}$.

Equations (3.4) and (3.7) solve the problem in the Hartree limit for the entire range $\infty > \tau > -\infty$ or $0 < \theta < \infty$. These results for entropy and energy as functions of τ are shown by the curves labeled "∞" in Figs. 2 and 1, respectively. As noted above, they simplify for $\tau \gg 1$. Simple limiting expressions can be obtained not only for $\tau \gg 1$, as noted above, but also for $\tau \ll -1$, where we find

$$\theta(\tau \ll -1) = -\tau + 1/4\theta^2$$

$$\simeq -\tau + 1/4\tau^2$$

$$= \theta_{\text{MF}} + 1/4\tau^2 , \tag{3.10}$$

and have identified the mean-field entropy function

$$\theta_{\text{MF}} = |\tau| . \tag{3.11}$$

The corresponding energy is

$$E_\infty(\tau \ll -1) \simeq -\tau^2/4 + 1/8|\tau|$$

$$= E_{\text{MF}} + 1/8|\tau| , \tag{3.12}$$

with the mean-field energy identified as

$$E_{\text{MF}} = -\tfrac{1}{4}\tau^2 . \tag{3.13}$$

Equations (3.11) and (3.13) are shown in Figs. 2 and 1 by the dashed straight line and parabola, respectively. We note in Eq. (3.12) that the first correction to the asymptotic energy is smaller by the factor $|\tau|^{-3}$, and not by $|\tau|^{-3/2}$, as might be expected from Eq. (3.9) and the discussion

which follows it. We shall see in Secs. IV and V that this is a natural consequence of the isotropy of the model. Because the quartic interaction depends only upon the "radial" component of the field, $\phi = (\sum \phi_i^2)^{1/2}$, the $\tau^{1/2}$ correction to the energy comes from this one degree of freedom alone, and contributes to E_n only in order n^{-1}. It consequently disappears from E_∞. The difference $E_n - E_\infty$ is plotted in Fig. 4 for $n = 1$, 2, 3, and 4.

The specific heat per degree of freedom in the Hartree limit, C_∞, is obtained by differentiating θ with respect to τ. It is convenient to work instead with the variable κ and to obtain from Eq. (3.4) the derivative

$$\frac{d\tau}{d\kappa} = 2\kappa + \frac{1}{2\kappa^2} = \frac{\kappa_2^2}{2\kappa},$$
(3.14)

where

$$\kappa_2 = (4\kappa^2 + \kappa^{-1})^{1/2}$$
(3.15)

is the inverse correlation length for energy fluctuations, as will be discussed in Sec. VII below. Figure 5 shows κ_2, 2κ, and the ration $2\kappa/\kappa_2$ plotted vs τ. From Eqs. (3.14) and (3.15) one finds[13]

$$C_\infty = -2\frac{d^2 E_\infty}{d\tau^2} = -\frac{d\theta}{d\tau}$$

$$= -\frac{d}{d\tau}\frac{1}{2\kappa} = \frac{1}{2\kappa^2}\frac{d\kappa}{d\tau}$$

$$= \frac{1}{\kappa\kappa_2^2} = \frac{1}{1+4\kappa^3}.$$
(3.16)

This is the smooth monotonic function of τ shown by the curve labeled ∞ in Fig. 3. It has expansions outside the critical region of the form

$$C_\infty = \begin{cases} \frac{1}{4}\tau^{-3/2} - \frac{1}{4}\tau^{-3} + \cdots, & \tau \gg 1 \\ 1 - \frac{1}{2}|\tau|^{-3} + \cdots, & \tau \ll -1 \end{cases}$$
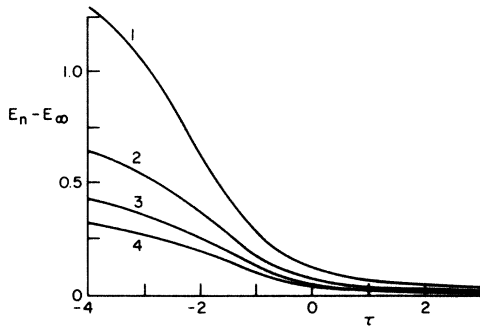(3.17)

FIG. 4. Deviation of the free-energy density from the Hartree limit, $E_n - E_\infty$, vs reduced temperature τ, for $n = 1$, 2, 3, and 4.

as can also be obtained by direct differentiation of Eq. (3.8) or Eq. (3.9).

IV. QUANTUM-MECHANICAL EQUIVALENCE

In this section we review the equivalence of the transfer matrix of statistical mechanics to the unitary time-development operator of quantum mechanics. This equivalence has already been discussed in detail[14]; we will therefore content ourselves here with a brief summary. The equivalence is easily exhibited by means of an analytic continuation of the space variable u into the complex plane as the pure imaginary quantity $u = it$, with t the analog of the time variable in the quantum-mechanical evolution of the oscillator. The extent of the system becomes the imaginary quantity $\Omega = i(t_2 - t_1) = it_{21}$ and the partition function becomes

$$Z_{it_{21}} = \int \delta\phi \exp\left(i \int_{t_1}^{t_2} dt\, L\right).$$
(4.1)

The Lagrangian now assumes the usual form of the difference between kinetic and potential energies,

$$L = \frac{1}{2}\left(\frac{\partial\phi}{\partial t}\right)^2 - V(\phi),$$
(4.2)

with potential energy

$$V(\phi) = \frac{1}{2}\tau\phi^2 + \frac{1}{4}\phi^4.$$
(4.3)

For the sake of simplicity, we limit ourselves for the moment to a single-component field.

The functional integral in Eq. (4.1) is nothing other than the Feynman sum over paths, which can be expressed in terms of $\mathcal{H}$, the Hamiltonian, as the trace
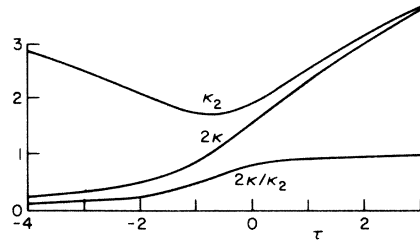

FIG. 5. Reciprocal correlation lengths vs reduced temperature τ. κ^{-1} and κ_2^{-1} are the correlation lengths for the order parameter and the square of the order parameter, respectively. The minimum in κ_2 corresponds to the phase transition which occurs in higher-dimensional systems, but which is smeared out by fluctuations in one dimension. In the absence of anharmonic interaction, κ_2 would be equal to 2κ. With anharmonicity taken into account, the ratio $2\kappa/\kappa_2$ varies monotonically between the limits 0 and 1.

$$Z_{it_{21}} = (\text{const.}) \times \text{Tr} e^{-it_{21} \mathcal{K}} .$$ (4.4)

We now analytically continue back to real values of u and find that the desired function is given in the thermodynamic limit by the quantum-mechanical ground-state-energy eigenvalue E:

$$Z_\Omega = (\text{const.}) \times \text{Tr} e^{-\Omega \mathcal{K}}$$

$$\simeq (\text{const.}) \times e^{-\Omega E} .$$ (4.5)

By substitution of Eq. (4.5) into Eq. (1.9) it is evident that the ground-state energy appearing in Eq. (4.5) is identical to the E of Eq. (2.6). The last line of Eq. (4.5) follows from the fact that in the thermodynamic limit ($\Omega \to \infty$), contributions to the trace from excited states become negligibly small compared to the ground-state contribution. The Hamiltonian function which appears in the above equations is that of a one-dimensional anharmonic oscillator,

$$\mathcal{K} = -\frac{1}{2} \frac{\partial^2}{\partial \phi^2} + V(\phi) .$$ (4.6)

All of the above is readily generalized to an n-component field. Because of the isotropy of the model, the Hamiltonian can be written in terms of the radial and angular variables. The dependence on the angle coordinates can be dropped from the Hamiltonian function, as we are only interested in the ground state. Thus there remains only the dependence on the radial coordinate ϕ,

$$\mathcal{K}_n = -\frac{1}{2}\left(\frac{\partial^2}{\partial \phi^2} + \frac{n-1}{\phi}\frac{\partial}{\partial \phi}\right) + V_n(\phi) .$$ (4.7)

Here the dependence on the dimension n appears in both the potential-energy and the kinetic-energy terms. It is convenient to transfer all of the n dependence to the potential energy term by transforming to the new operator

$$H_n \equiv \phi^\nu \mathcal{K}_n \phi^{-\nu}$$

$$= -\frac{1}{2}\left[\left(\frac{\partial}{\partial \phi} - \frac{\nu}{\phi}\right)^2 + \frac{n-1}{\phi}\left(\frac{\partial}{\partial \phi} - \frac{\nu}{\phi}\right)\right] + V_n$$

$$= -\frac{1}{2}\left(\frac{\partial^2}{\partial \phi^2} + \frac{n-1-2\nu}{\phi}\frac{\partial}{\partial \phi}\right) + \frac{n\nu - \nu^2 - 2\nu}{2\phi^2} + V_n .$$ (4.8)

Choosing 2ν equal to n plus a constant eliminates the n dependence from the coefficient of the first-order differential operator. The specific choice $2\nu = n - 1$ eliminates this term altogether and leaves us with the effectively one-dimensional Hamiltonian

$$H_n = -\frac{1}{2}\frac{\partial^2}{\partial \phi^2} + U_n(\phi) .$$ (4.9)

The new potential includes a kind of "centrifugal" term

$$U_n(\phi) = \frac{l(l+1)}{2\phi^2} + U_n(\phi)$$

$$= \frac{l(l+1)}{2\phi^2} + \frac{\tau}{2}\phi^2 + \frac{1}{4n}\phi^4$$ (4.10)

associated with the "angular momentum"

$$l = \nu - 1 = (n-3)/2 .$$ (4.11)

Because of the factor ϕ^{l+1} in the transformation in Eq. (4.8) the eigenfunction of H_n must vanish at $\phi = 0$. This boundary condition applies for all $n > 1$. Equations (4.9) and (4.10) can be interpreted as meaning that the ground-state problem for arbitrary n has been transferred to the problem of computing the excited states of the three-dimensional model corresponding to various values of l. (See Ref. 2 for another discussion of this equivalence.) According to Eq. (4.11), l can formally be extended to half-odd-integer values. l even becomes a continuous variable if n is regarded as such. But returning now to integer l and letting $nE_{n,l}$ represent the lth excited-state energy of an n-dimensional oscillator, we use Eqs. (4.8) and (4.9) to obtain the connection between $E_{3,l}$ and the ground-state eigenvalue E_n, where $n = 3 + 2l$. To make this connection exact, we have to allow for the minor complication of the differing normalization of the anharmonic term. We take this into account by scaling the order parameter to $\phi' = (3/n)^{1/6}\phi$. Then Eq. (4.9) becomes

$$H_n = -\frac{1}{2}\frac{\partial^2}{\partial \phi^2} + \frac{l(l+1)}{2\phi^2} + \frac{\tau}{2}\phi^2 + \frac{1}{4n}\phi^4$$

$$= \left(\frac{3}{n}\right)^{1/3}\left[-\frac{1}{2}\frac{\partial^2}{\partial \phi'^2} + \frac{l(l+1)}{2\phi'^2}\right.$$

$$\left. + \left(\frac{n}{3}\right)^{2/3}\frac{\tau}{2}\phi'^2 + \frac{1}{12}\phi'^4\right] .$$ (4.12)

The desired connection between the eigenvalues is therefore

$$E_n(\tau) = (3/n)^{4/3} E_{3,(n-3)/2}[(n/3)^{2/3}\tau] .$$ (4.13)

This kind of reduction can also be applied to the $n = 3$ ground state itself. We see this from the fact that $l(l+1) = 0$ for $n = 3$, according to Eq. (4.11). Consequently the centrifugal term disappears in this case, and both $n = 3$ and $n = 1$ involve finding eigenvalues of essentially the same operator, Eq. (4.9). The only substantial difference in the two cases is in the boundary condition at $\phi = 0$, so that the ground-state eigenvalue for $n = 3$ is in fact the first-excited-state eigenvalue for the $n = 1$ prob-

lem. Here we scale the order parameter to ϕ' $= 3^{-1/6}\phi$, in order to allow for the difference in anharmonic normalization, obtaining

$$E_3(\tau) = 3^{-4/3}E_{1,1}(3^{2/3}\tau).\qquad(4.14)$$

The $n = 1$ ground-state energy and the reciprocal of the $n = 1$ excitation energy are displayed by the curves labeled "REAL" in Figs. 2 and 6, respectively, of Ref. 6. From these sources and Eq. (4.14) as well as from further numerical computations, we have prepared the curves labeled $n = 1$ and $n = 3$ in Fig. 1 of the present paper.

The ground-state problem for arbitrary n can alternatively be reduced to the problem of finding excitation energies for the two-dimensional instead of for the three-dimensional model. For this reduction we return to Eq. (4.8) and choose

$$\nu = (n-2)/2.\qquad(4.15)$$

Distinguishing the operator which we thereby obtain by a prime, we have

$$H_n' = -\frac{1}{2}\left(\frac{\partial^2}{\partial\phi^2}+\frac{1}{\phi}\frac{\partial}{\partial\phi}\right)+W_n(\phi),\qquad(4.16)$$

where the new potential

$$W_n(\phi) = \frac{\nu^2}{2\phi^2}+V_n(\phi)$$

$$= \frac{\nu^2}{2\phi^2}+\frac{\tau}{2}\phi^2+\frac{1}{4n}\phi^4\qquad(4.17)$$

contains a two-dimensional centrifugal potential term corresponding to the planar angular momentum ν. Here again, as with the three-dimensional oscillator, the correspondence to excited states can be extended formally so that ν takes on not only integer values, but half-odd-integer and continuous values as well. In both models only the excited states associated with eigenfunctions having no radial nodes correspond to the ground-state energies of the higher-dimensional oscillators.

Allowing for the change of the anharmonic normalization in Eq. (4.17), in analogy with the derivation of Eq. (4.13), gives for the eigenvalue of Eq. (4.16) the connection

$$E_n(\tau) = (2/n)^{4/3}E_{2,(n-2)/2}[(n/2)^{2/3}\tau].\qquad(4.18)$$

For the special case $n = 4$, Eq. (4.18) reduces to

$$E_4(\tau) = 2^{-4/3}E_{2,1}(2^{2/3}\tau).\qquad(4.19)$$

We have applied this equation in the preparation of Fig. 1. The $n = 2$ ground-state energy and the reciprocal of the $n = 2$ excitation energy are dis-

played by the curves labeled "COMPLEX" in Figs. 2 and 6, respectively, of Ref. 6. Allowing for a further scaling, because of the n-independent normalization of the anharmonic term in Ref. 6, we have used this material and further numerical computations to prepare the curves labeled $n = 2$ and $n = 4$ in Fig. 1.

Although no use of it will be made in this paper, we note here in passing that the connection between the ground-state energy E_n and the excited-state energy $E_{n_0,(n-n_0)/2}$ which is illustrated by Eqs. (4.18) and (4.13) for $n_0 = 2$ and 3, respectively, can be generalized to $n_0 > 3$.

V. CORRECTION TO THE HARTREE APPROXIMATION

In order to obtain systematic corrections[15] to the Hartree approximation as an expansion in powers of n^{-1}, we return to the effective one-dimensional problem defined by Eqs. (4.9) and (4.10). A typical example of the effective radial potential $U_n(\phi)$ is shown in Fig. 6. Here we have chosen $\tau = 2$ and $n = 5$, so that $l = (n-3)/2 = 1$. The curves show separately the harmonic potential $\tau\phi^2/2 = \phi^2$, the centrifugal potential $l(l+1)/2\phi^2 = \phi^{-2}$, and the sum of the two, which has a minimum of $U_n(1)$ $= 2$ at $\phi^2 = 1$. At the minimum the anharmonic term equals $(4n)^{-1} = \frac{1}{20}$ or only 2.5% of the total potential. It has therefore been neglected. As we need to calculate the ground-state eigenvalue for the Hamiltonian operator of Eq. (4.9), it is natural to approximate $U_n(\phi)$ by a parabola centered at the minimum and matching the curvature at that point. This approximation is also shown in Fig. 6 (by a dashed curve), and reduces the eigenvalue
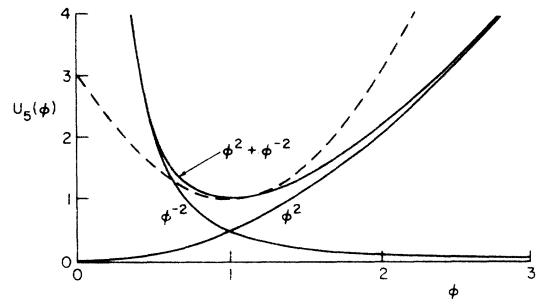

FIG. 6. Effective quantum-mechanical potential U_5 vs order parameter ϕ for $\tau = 2$ and $n = 5$. For this choice of reduced temperature and oscillator dimensionality, the anharmonic term can be neglected. The harmonic and centrifugal terms are shown by the curves labeled ϕ^2 and ϕ^{-2}, respectively. The parabolic fit to the sum is illustrated by the dashed line. The quantum-mechanical zero-point energy calculated in this parabolic approximation is an important contribution to the first-screening-approximation correction.

problem to that of the harmonic oscillator. Carrying this out for arbitrary n and $\tau \gg 1$, for which we are still permitted to neglect the anharmonic term, gives a potential minimum at ϕ_m, determined by

$$\phi_m^4 = l(l+1)/\tau . \tag{5.1}$$

The value of the potential at the minimum is

$$\begin{aligned} \overline{U}_n(\phi_m) &= [\tau l(l+1)]^{1/2} \\ &= \tfrac{1}{2}n\tau^{1/2}(1-3/n)^{1/2}(1-1/n)^{1/2} \\ &\simeq \tfrac{1}{2}n\tau^{1/2} - \tau^{1/2} , \end{aligned} \tag{5.2}$$

to $O(1)$. The bar on U_n indicates the neglect of anharmonicity.

The curvature at the minimum is

$$\overline{U}_n''(\phi_m) = 3\, l(l+1)/\phi_m^4 + \tau = 4\tau . \tag{5.3}$$

We find the ground-state energy by adding to the potential at the minimum the zero-point energy:

$$\begin{aligned} nE_n(\tau) &= \overline{U}_n(\phi_m) + \tfrac{1}{2}[\overline{U}_n''(\phi_n)]^{1/2} \\ &= \overline{U}_n(\phi_m) + \tau^{1/2} = \tfrac{1}{2}n\tau^{1/2} . \end{aligned} \tag{5.4}$$

The zero-point energy has exactly canceled the n^{-1} correction to the potential energy, yielding a net energy exactly proportional to n. This is the result to be expected in the absence of interaction and is in agreement with Eq. (2.7). The corresponding ground-state wave function ψ_n is a Gaussian function centered at ϕ_m. Substituting from Eq. (5.3), we obtain

$$\psi_n \propto e^{-(\overline{U}'')^{1/2}|(\phi-\phi_m)^2/2} \simeq e^{-\tau^{1/2}(\phi-\phi_m)^2} . \tag{5.5}$$

Squaring this, we get a probability distribution of exactly the form of Eq. (2.24). An apparent discrepancy occurs in the location of the maximum of the distribution, because from Eq. (5.1) we obtain to $O(1)$

$$\begin{aligned} \phi_m^2 &= \frac{n}{2\tau^{1/2}}\left(1-\frac{3}{n}\right)^{1/2}\left(1-\frac{1}{n}\right)^{1/2} \\ &\simeq \frac{n-2}{2\tau^{1/2}} , \end{aligned} \tag{5.6}$$

as compared to $\phi_{\min}^2 = (n-1)/2\tau^{1/2}$ in Eq. (2.18). Thus $\phi_{\min} \neq \phi_m$ and it is necessary to distinguish between the maximum of the distribution and the minimum of the potential. This discrepancy can be resolved by noting that the skewness of $U_n(\phi)$ causes it to deviate sufficiently from the symmetrical parabolic approximation to shift the maximum outwards from ϕ_m to the slightly larger value $\phi_{\min}$. We will return to this point again in Sec. VI below.

Having now demonstrated that the simplification of stochastic peaking which was worked out in

Sec. II can be recovered in the quantum-mechanical formulation of the problem, we employ again the parabolic fit to the potential—but this time including the anharmonic potential in the total potential to be fitted. This will enable us to obtain results in the range $n \gg 1$ which are valid for all values of τ. With the anharmonic term included, the minimum is determined by

$$U_n'(\phi_m) = -\frac{l(l+1)}{\phi_m^3} + \tau\phi_m + \frac{1}{n}\phi_m^3 = 0 . \tag{5.7}$$

The curvature is

$$\begin{aligned} U_n''(\phi_m) &= 3\,\frac{l(l+1)}{\phi_m^4} + \tau + \frac{3}{n}\phi_m^2 \\ &= 4\,\frac{l(l+1)}{\phi_m^4} + \frac{2}{n}\phi_m^2 \\ &\simeq 1/\theta^2 + 2\theta = 4\kappa^2 + \kappa^{-1} = \kappa_2^2 , \end{aligned} \tag{5.8}$$

where κ_2 has been defined in Eq. (3.15) and is discussed in Sec. VII below. In Eq. (5.8) we have approximated Eq. (5.7) by Eq. (3.3) and we have substituted $\phi_m^2 \simeq n\theta$ and $l(l+1) \simeq n^2/4$ into Eq. (5.8). This last approximation is sufficiently accurate for Eq. (5.8), it being of $O(1)$. But for computing the potential minimum $U_n(\phi_m)$ we need the more accurate expression $l(l+1) \simeq n^2/4 - n$. We can still use $\phi_m^2 \simeq n\theta$, however, as the resulting error in $U_n(\phi_m)$ by virtue of Eq. (5.7) is of the order of $[\phi_m - (n\theta)^{1/2}]^2 = (\phi_m^2 - n\theta)^2/[\phi_m + (n\theta)^{1/2}]^2$ or $O(n^{-1})$. Thus we obtain to $O(1)$

$$\begin{aligned} U_n(\phi_m) &\simeq \frac{1}{2\phi_m^2}\left(\frac{n^2}{4}-n\right) + \frac{\tau}{2}\phi_m^2 + \frac{1}{4n}\phi_m^4 \\ &\simeq n\left(\frac{\tau}{2}\theta + \frac{1}{4}\theta^2 + \frac{1}{8\theta}\right) - \frac{1}{2\theta} \\ &= nE_\infty - 1/2\theta = nE_\infty - \kappa . \end{aligned} \tag{5.9}$$

Adding the zero-point energy to this gives

$$\begin{aligned} nE_n &= nE_\infty - 1/2\theta + \tfrac{1}{2}[U_n''(\phi_m)]^{1/2} \\ &= nE_\infty + (1/2\theta)[-1 + 1(1+2\theta^3)^{1/2}] , \end{aligned} \tag{5.10}$$

which can also be expressed in terms of the inverse correlation lengths as

$$E^{(1)} = n(E_n - E_\infty) = \tfrac{1}{2}(\kappa_2 - 2\kappa) . \tag{5.11}$$

This result is shown by the curve labeled "s" in Fig. 7. The curves labeled 1, 2, 3, and 4 there exhibit the corresponding numerical solutions for these values of n.

We note that for $\tau \gg 1$, $\kappa_2 \simeq 2\kappa$, according to Eq. (3.15), so that the two contributions to Eq. (5.11) cancel, just as we saw above in Eq. (5.4) when

neglecting the anharmonic term in the potential. The leading terms in the n^{-1} correction to E_n in this region are [from Eq. (3.5a)]

$$E^{(1)} \simeq \tfrac{1}{8}\kappa^{-2} - \tfrac{1}{128}\kappa^{-5} \simeq \tfrac{1}{8}\kappa_0^{-2} - \tfrac{9}{128}\kappa_0^{-5}$$

$$= \tfrac{1}{8}\tau^{-1} - \tfrac{9}{128}\tau^{-5/2}, \qquad (5.12)$$

while for $\tau \ll -1$ we find from Eqs. (5.11) and (3.5b)

$$E^{(1)} \simeq \tfrac{1}{2}\kappa^{-1/2} - \kappa \simeq \tfrac{1}{2}(2|\tau|)^{1/2} - 1/2|\tau|, \qquad (5.13)$$

where $2|\tau|$ will be recognized as the stiffness in this limiting region, where the centrifugal contribution to $U_n(\phi)$ can be neglected. Equation (5.13) supplies the expected $|\tau|^{1/2}$ correction to the energy, which we remarked above was missing from the Hartree energy, Eq. (3.12).

Differentiating Eq. (5.10), we find the correction to the entropy function

$$\theta^{(1)} = n(\theta_n - \theta) = 2n\frac{d(E_n - E_\infty)}{d\tau}$$

$$= \frac{d\theta}{d\tau}\frac{d}{d\theta}\frac{1}{\theta}[-1 + (1 + 2\theta^3)^{1/2}]$$

$$= \frac{d\theta}{d\tau}\frac{1}{2\theta^2}[(1 + 2\theta^3)^{1/2} + 2 - 3(1 + 2\theta^3)^{-1/2}].$$

$$(5.14)$$

The remaining derivative is the negative of the Hartree specific heat,

$$\frac{d\theta}{d\tau} = -C_\infty = -\frac{2\theta^3}{1 + 2\theta^3} = -1 + (1 + 2\theta^3)^{-1}, \qquad (5.15)$$

as exhibited in Eq. (3.16) and as displayed by the curve labeled "∞" in Fig. 3. It is convenient to divide Eq. (5.14) by θ, which gives us the fractional correction to the Hartree entropy function.
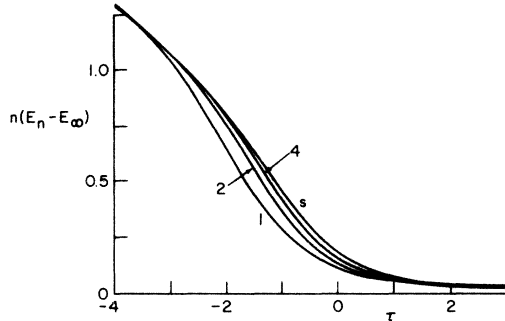
Collecting powers of $(1 + 2\theta^3)^{-1/2} = 2\kappa/\kappa_2$, we find

$$-\theta^{(1)}/\theta = n(1 - \theta_n/\theta)$$

$$= (1 + 2\theta^3)^{-1/2} + 2(1 + 2\theta^3)^{-1} - 3(1 + 2\theta^3)^{-3/2},$$

$$(5.16)$$

which is shown by the curve labeled "s" in Fig. 8. The curves labeled $n = 1$, 2, 3, and 4 show the results of numerical computation, i.e., the results of differentiating the corresponding curves in Fig. 7. For $|\tau| \gg 1$ Eq. (5.16) reduces to

$$-\frac{\theta^{(1)}}{\theta} \simeq \begin{cases} 1/2\tau^{3/2}, & \tau \gg 1 \\ 1/\sqrt{2}|\tau|^{3/2}, & \tau \ll -1. \end{cases} \qquad (5.17)$$

Thus, aside from a factor of $\sqrt{2}$, the fractional entropy change has symmetrical asymptotic behavior.

Turning now to the specific heat, we differentiate Eq. (5.16) to find the $O(n^{-1})$ correction,

$$C^{(1)} = n(C_n - C_\infty) = \frac{d}{d\tau}n(\theta_n - \theta)$$

$$= -\frac{d\theta}{d\tau}\frac{d}{d\theta}\theta n\left(1 - \frac{\theta_n}{\theta}\right)$$

$$= \tfrac{1}{2}(1 + 2\theta^3)^{-1/2} + 4(1 + 2\theta^3)^{-1} - \tfrac{25}{2}(1 + 2\theta^3)^{-3/2}$$

$$- 10(1 + 2\theta^3)^{-2} + \tfrac{51}{2}(1 + 2\theta^3)^{-5/2} + 6(1 + 2\theta^3)^{-3}$$

$$- \tfrac{27}{2}(1 + 2\theta^3)^{-7/2}. \qquad (5.18)$$

Equation (5.18) and the numerical computations are shown in Fig. 9. Equation (5.21) reduces for $|\tau| \gg 1$ to

$$C^{(1)} \simeq \begin{cases} -\tfrac{1}{2}\tau^{-3}, & \tau \gg 1 \\ \tfrac{1}{4}\sqrt{2}|\tau|^{-3/2}, & \tau \ll 1 \end{cases} \qquad (5.19)$$
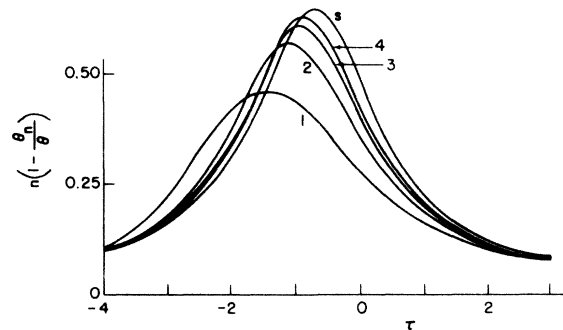

FIG. 7. Deviation of the free energy from the Hartree limit, $n(E_n - E_\infty)$, vs reduced temperature τ. The cases $n = 1$, 2, and 4 show the tendency toward the first screening correction (curve labeled "s") $E^{(1)}(\tau)$ in the limit $n \to \infty$. (The curve for $n = 3$ falls too close to that for $n = 4$ to be included.)

FIG. 8. Fractional entropy reduction vs reduced temperature τ. $\theta - \theta_n$ is the reduction of the entropy function from its Hartree value, θ. The cases $n = 1$, 2, 3, and 4 show the tendency toward the first screening correction (curve labeled "s") in the limit $n \to \infty$.

as expected from direct differentiation of Eq.
(5.17) or Eqs. (5.12) and (5.13). Comparison of
Eq. (5.19) with Eq. (3.17) shows that the τ depen-
dence of the n^{-1} correction to the specific heat
dominates for sufficiently large negative τ. This
ensures a maximum in the specific heat, located
for $n \gg 1$ at

$$\tau_{max} = -2n^{2/3}, \tag{5.20}$$

of magnitude

$$C_{max} = 1 + \tfrac{1}{16} n^{-2}. \tag{5.21}$$

The computer calculations for small positive inte-
ger values of n show a maximum which is more
pronounced than would be indicated by Eq. (5.21).
Truncation of the series expansion at $O(n^{-1})$ im-
plies only qualitative validity for small n. The
requirement of positive definiteness for specific
heat, or convexity for the energy,[16] puts an abso-
lute lower bound on n. Figure 10 shows the ratio
$C^{(1)}/C_\infty$ as a function of τ. The minimum of -1.24
falls at $\tau \simeq 0$, which would lead to a negative spe-
cific heat in this vicinity for values of n smaller
than the minimum ratio. Therefore, the convexity
theorem permits the use of the first-order screen-
ing approximation only for $n \geq 1.24$, or if we limit
n to integer values, for

$$n \geq 2. \tag{5.22}$$

VI. HIGHER-ORDER CORRECTIONS

In this section we derive the corrections to the
free-energy density which are of order n^{-1}. These
are of relative order n^{-2} compared to the Hartree
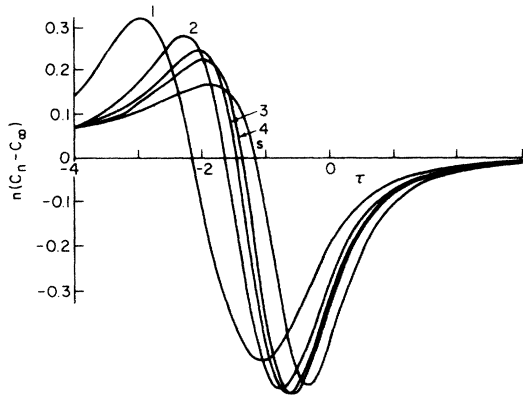contribution to the free energy and of $O(n^{-1})$ rela-
tive to the correction which has been calculated
in Sec. V. The first effect which we need to ex-
amine is the discrepancy noticed in Sec. V in
connection with Eq. (5.6). There we noted that the
maximum of the wave function determined in the
quantum-mechanical problem occurred at a small-
er value of the order parameter than found in
Eq. (2.18) for the equivalent stochastic problem
studied in Sec. II. We remarked that the reason
for the discrepancy was that the potential contained
some skewness which was neglected in the par-
abolic fit used for the quantum-mechanical cal-
culation. This skewness is illustrated in Fig. 6
by the deviation of the solid from the dashed
curve, and we now proceed to take it into account
by returning to Eq. (4.9) and expanding the poten-
tial of Eq. (4.10) to higher order. It will be suffi-
cient for our present purposes to truncate this
Taylor-series expansion at fourth order, which
gives us the approximation

$$H_n \simeq U_n(\phi_m) - \frac{1}{2} \frac{\partial^2}{\partial \phi^2} + \tfrac{1}{2} U''(\phi_m)(\phi - \phi_m)^2$$

$$+ \frac{1}{3!} U'''(\phi_m)(\phi - \phi_m)^3 + \frac{1}{4!} U^{iv}(\phi_m)(\phi - \phi_m)^4. \tag{6.1}$$

For the purpose of clearing up the discrepancy
in the location of the maximum of the wave func-
tion, we concentrate first on the simplified prob-
lem which is obtained by neglecting the anharmonic
term in the potential. This simplified potential,
designated as before by a bar, is given by

$$\bar{U}_n(\phi) = l(l+1)/2\phi^2 + \tfrac{1}{2}\tau\phi^2. \tag{6.2}$$

FIG. 9. Deviation of the specific heat C_n from the
Hartree limit C_∞ vs reduced temperature τ. The cases
$n = 1$, 2, 3, and 4 show the tendency toward the first-
screening-approximation correction (curve labeled "s")
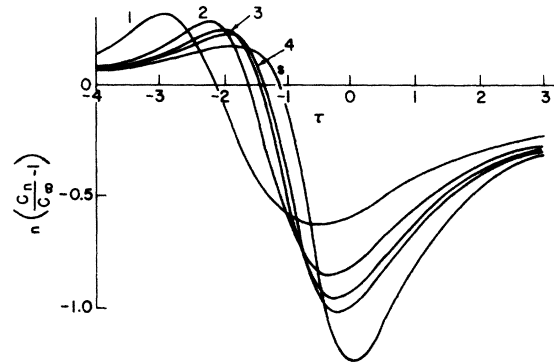in the limit $n \to \infty$.

FIG. 10. Fractional deviation of the specific heat from
the Hartree value. The cases $n = 1$, 2, 3, and 4 tend
toward the curve labeled "s", which shows $-2C_\infty^{-1}\partial^2 E^{(1)}/\partial\tau^2$, the ratio of the first-screening-approximation cor-
rection to the Hartree specific heat C_∞. The minimum
of -1.24 in the latter implies that the first screening
approximation violates the positive definiteness of the
specific heat for $n < 1.24$.

The value of this potential at its minimum has already been given in Eq. (5.2) and the location of the minimum is determined by Eq. (5.1). The curvature is expressed by Eq. (5.3) and the higher-order derivatives occuring in Eq. (6.1) are

$$\overline{U}''' = -12\frac{l(l+1)}{\phi_m^5} = -\frac{12\tau}{\phi_m} \simeq -\frac{12\sqrt{2}}{n^{1/2}}\kappa^{5/2},\qquad (6.3)$$

$$\overline{U}^{\text{iv}} = 60\frac{l(l+1)}{\phi_m^6} = \frac{60\tau}{\phi_m^2} \simeq \frac{120}{n}\kappa^3.\qquad (6.4)$$

We are thus led to the quantum-mechanical problem of finding the lowest eigenvalue of the operator

$$H_n \simeq \overline{U}_n(\phi_m) + 2\kappa\overline{H}_n^{\text{red}}\qquad (6.5)$$

where the reduced Hamiltonian has the form

$$\overline{H}_n^{\text{red}} = -\frac{1}{2}\frac{\partial^2}{\partial q^2} + \frac{1}{2}q^2 - \lambda q^3 + \lambda'q^4.\qquad (6.6)$$

We have introduced the reduced coordinate

$$q = (2\kappa)^{1/2}(\phi - \phi_m)\qquad (6.7)$$

and the dimensionless coupling constants for the cubic and quartic terms,

$$\lambda = -(1/3!)(2\kappa)^{-5/2}\overline{U}''' = 1/2n^{1/2},\qquad (6.8)$$

$$\lambda' = (1/4!)(2\kappa)^{-3}\overline{U}^{\text{iv}} = 5/8n.\qquad (6.9)$$

The shift in the maximum is produced entirely by the cubic term, as the quartic term preserves the symmetry of the parabolic approximation. To calculate the shift in the maximum we need the first-order perturbation in the ground-state wave function,

$$\Delta\psi_0 = -\lambda\sum_{n=1}^{\infty}\frac{(q^3)_{n0}}{E_0 - E_n}\psi_n$$

$$= \lambda[(q^3)_{10}\psi_1 + \tfrac{1}{3}(q^3)_{30}\psi_3]$$

$$\simeq \lambda q\,\psi_0.\qquad (6.10)$$

The unperturbed spectrum of the reduced Hamiltonian is $E_n = n + \frac{1}{2}$. ψ_n are the associated orthonormal eigenfunctions. The approximation of the last line of Eq. (6.10) is valid for $q \ll 1$. The ground-state wave function is the Gaussian

$$\psi_0(q) = \pi^{-1/4}e^{-q^2/2},\qquad (6.11)$$

so that for $\lambda \ll 1$ we find the shift in maximum to be

$$\Delta q = \lambda.\qquad (6.12)$$

Returning to Eq. (6.7) we find that the shift in the location of the maximum in the order parameter relative to the parabolic approximation is

$$\Delta\phi_m = (4\tau)^{-1/4}\Delta q = 1/4\phi_m\tau^{1/2}.\qquad (6.13)$$

Consequently, neglecting terms which are quadratic in the shift, we find for the square of the order parameter at the maximum

$$(\phi_m + \Delta\phi_m)^2 \simeq \phi_m^2 + 2\phi_m\Delta\phi_m$$

$$= (n-2)/2\tau^{1/2} + 1/2\tau^{1/2}$$

$$= (n-1)/2\tau^{1/2}.\qquad (6.14)$$

We have substituted from Eq. (5.6), and it is evident that the asymmetry of the potential does restore agreement between the quantum-mechanical treatment of the problem in Sec. V and the stochastic treatment given in Sec. II.

It is instructive to carry further the comparison between the quantum-mechanical and the stochastic treatments of Secs. V and II, respectively, by calculating the shift to $O(n^{-1})$ in the free energy. Here we know from the stochastic treatment that we are really dealing with n independent degrees of freedom without any interaction between them. Consequently, the total free energy is exactly proportional to n and there are in fact no terms of order unity, or of order n^{-1} or higher in n^{-1}. Thus, if the quantum-mechanical treatment is carried out accurately, it must follow that all such higher-order contributions cancel in the final answer. We briefly sketch how this happens, as a prototype for the subsequent more complicated calculation which includes anharmonicity. First, we note that the reduced Hamiltonian gets its ground-state energy shifted by second-order perturbation from the cubic term and by first-order perturbation from the quartic term. These two contributions are of the same order and combine to give

$$\Delta\overline{E}_G^{\text{red}} = -\tfrac{11}{8}\lambda^2 + \tfrac{3}{4}\lambda'$$

$$= (1/32n)(-11+15) = 1/8n.\qquad (6.15)$$

Consequently the second term in Eq. (6.5), including the unperturbed zero-point energy, is

$$2\kappa\overline{E}_G^{\text{red}} = \kappa + \kappa/4n$$

$$\simeq \tau^{1/2} + (1/4n)\tau^{1/2}.\qquad (6.16)$$

Now we must calculate to $O(n^{-1})$ the first term in Eqs. (6.5), namely, the potential evaluated at its minimum. The location of the minimum is given in Eq. (5.1), which in turn leads to

$$\overline{U}_n(\phi_m) = \frac{l(l+1)}{2\phi_m^2} + \frac{\tau\phi_m^2}{2}$$

$$= \tau\phi_m^2 = [\tau l(l+1)]^{1/2}$$

$$= \frac{n}{2}\tau^{1/2}\left(1 - \frac{1}{n}\right)^{1/2}\left(1 - \frac{3}{n}\right)^{1/2}$$

$$\simeq \frac{n}{2}\tau^{1/2}\tau^{1/2} - \frac{1}{4n}\tau^{1/2}.\qquad (6.17)$$

Here we have terminated the expansion at $O(n^{-1})$. Substituting Eqs. (6.17) and (6.16) into Eq. (6.5) gives, for the ground-state eigenvalue of H_n,

$$E_n(\tau) = \bar{U}_n(\phi_n) + 2\tau^{1/2}\bar{E}_G^{\text{red}}$$

$$= \tfrac{1}{2}n\tau^{1/2} . \qquad (6.18)$$

We see that the required cancellation of higher-order terms has indeed occurred.

The effect of anharmonicity to $O(n^{-1})$ will now be calculated in the same way. (Of course, here we do not expect cancellation.) Just as before, we specify the deviation from the parabolic fit to the potential, which is shown for $n = 5$ and various values of τ in Fig. 11, by the third derivative

$$U''' = -12\frac{l(l+1)}{\phi_m^5} + \frac{6}{n}\phi_m$$

$$\simeq \frac{6\phi_m}{n}\left(1 - \frac{n^3}{2\phi_m^6}\right)$$

$$\simeq 6\left(\frac{\theta}{n}\right)^{1/2}\left(1 - \frac{1}{2\theta^3}\right)$$

$$= 3\left(\frac{2}{n\kappa}\right)^{1/2}(1 - 4\kappa^3) \qquad (6.19)$$

and the fourth derivative

$$U^{\text{iv}} = 60\frac{l(l+1)}{\phi_m^6} + \frac{6}{n} \simeq \frac{6}{n}\left(1 + \frac{5}{2}\frac{n^3}{\phi_m^6}\right)$$

$$\simeq \frac{6}{n}\left(1 + \frac{5}{2\theta^3}\right) = \frac{6}{n}(1 + 20\kappa^3) . \qquad (6.20)$$

The dimensionless variable is now

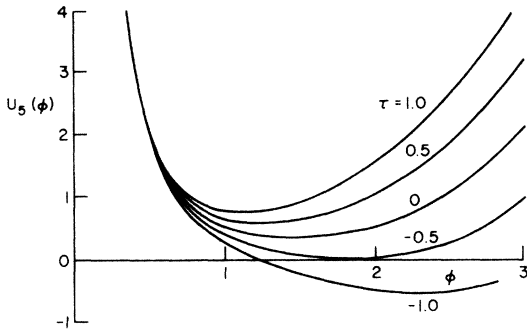$$q = \kappa_2^{1/2}(\phi - \phi_m) ; \qquad (6.21)$$

FIG. 11. Effective quantum-mechanical potential vs order parameter ϕ for $n = 5$ and various values of the reduced temperature τ. The case $\tau = 2$ is illustrated in Fig. 6, which also shows the parabolic fit to $U_5(\phi)$. As τ decreases the parabolic fit becomes worse and the skewness of $U_5(\phi)$ about its minimum becomes more marked. This effect contributes to the second screening approximation.

the dimensionless coupling constants for the cubic and quartic terms of the reduced Hamiltonian of Eq. (6.6) have become

$$\lambda = -(1/3!)\kappa_2^{-5/2}U'''$$

$$= (2n)^{-1/2}\kappa^{-1/2}\kappa_2^{-5/2}(4\kappa^3 - 1) , \qquad (6.22)$$

and

$$\lambda' = (1/4!)\kappa_2^{-3}U^{\text{iv}}$$

$$= (4n)^{-1}\kappa_2^{-3}(20\kappa^3 + 1) . \qquad (6.23)$$

The terms -1 and $+1$ inside the parentheses arise from the anharmonic term in the Ginzburg–Landau expression. Dropping them and replacing κ_2 by 2κ reduces Eqs. (6.22) and (6.23) to the earlier expressions, Eqs. (6.8) and (6.9), respectively. The cubic and quartic terms in H_n^{red} produce a shift in ground-state energy of

$$\kappa_2\Delta E_G^{\text{red}} = \kappa_2(-\tfrac{11}{8}\lambda^2 + \tfrac{3}{4}\lambda')$$

$$= n^{-1}\kappa_2^{-4}(-\tfrac{1}{2}\kappa^{-1} + 10\kappa^2 + 4\kappa^5) . \qquad (6.24)$$

Just as in Eq. (6.17), to the above quantum effect has to be added the correction to the minimum in the potential energy. This is purely a classical calculation and involves two effects. The first effect is the deviation of the centrifugal term from its ideal $n = \infty$ form, which we obtain as an expansion in powers of n^{-1}:

$$U_n((n\theta)^{1/2}) = \left(\frac{l(l+1)}{2\phi^2} + \frac{\tau}{2}\phi^2 + \frac{1}{4n}\phi^4\right)_{\phi=(n\theta)^{1/2}}$$

$$= \frac{n}{8\theta}\left(1 - \frac{3}{n}\right)\left(1 - \frac{1}{n}\right) + \frac{\tau}{2}n\theta + \frac{n}{4}\theta^2$$

$$= n\left[\frac{\tau}{2}\theta + \frac{1}{4}\theta^2 + \frac{1}{8\theta}\left(1 - \frac{4}{n} + \frac{3}{n^2}\right)\right]$$

$$= n\left(\frac{\tau}{2}\theta + \frac{1}{4}\theta^2 + \frac{1}{8\theta}\right) - \frac{1}{2\theta} + \frac{3}{8\theta}n^{-1}$$

$$= nE_\infty - \kappa + \tfrac{3}{4}\kappa n^{-1} . \qquad (6.25)$$

The first term in the above equation is simply the Hartree expression, Eq. (3.7), while the second term is the first correction to the Hartree expression, already found above in Eq. (5.9). The final term is a new correction of $O(n^{-1})$. For convenience, we have evaluated the potential at the approximate value $\phi = (n\theta)^{1/2}$. The actual potential minimum falls at a slightly different value of ϕ, which deviates from $(n\theta)^{1/2}$ by $\Delta\phi_n$, as determined by

$$U_n'' \Delta\phi_m + n/\phi_m^3 = 0 . \qquad (6.26)$$

The true minimum value of the potential is lower than that calculated in Eq. (6.25) by the amount

$$\Delta U_n = U_n(\phi_m) - U_n((n\theta)^{1/2}) = -\tfrac{1}{2} U_n''(\Delta\phi_m)^2$$

$$= -(n^2/2U_n'')(n\theta)^{-3} = -4\kappa^3/n\kappa_2^2, \qquad (6.27)$$

where $\Delta\phi$ has been substituted from Eq. (6.26). Adding the quantum correction of Eq. (6.24) to the classical corrections of Eqs. (6.25) and (6.27), we obtain, in analogy with Eq. (6.18),

$$\frac{3\kappa}{4n} + \Delta U_n + \kappa_2 E_G^{\text{red}} = \frac{1}{n\kappa_2^4}\left(\frac{1}{4\kappa} + 12\kappa^2\right). \qquad (6.28)$$

Unlike Eq. (6.18), however, this does not give the full correction of $O(n^{-1})$. In the present calculation an additional effect enters which was not encountered in the calculation earlier in this section. This is a correction to the zero-point energy arising from a change in the curvature at the minimum of the potential. This effect did not occur previously because, by virtue of Eqs. (5.1) and (5.3), the curvature at the potential minimum in the absence of anharmonicity is given exactly by $4\kappa^2 = 4\tau$, to all orders in n^{-1}. This is no longer the case when anharmonicity is present and we calculate the value of the curvature at the potential minimum in a fashion very similar to the way that we found the value of the potential itself in Eqs. (6.25) and (6.27). First, to $O(n^{-1})$, the curvature at the approximate location $\phi = (n\theta)^{1/2}$ is

$$U_n''((n\theta)^{1/2}) = \kappa_2^2 - 12\kappa^2/n. \qquad (6.29)$$

A further change arises because of the difference $\Delta\phi_m$ in the location of the potential minimum. This brings in the third derivative, so that substitution from Eqs. (6.19) and (6.26) gives

$$\Delta U_n'' = U_n''(\phi_m) - U_n''((n\theta)^{1/2})$$

$$= U_n''' \Delta\phi_m = (12\kappa/n\kappa_2^2)(4\kappa^3 - 1). \qquad (6.30)$$

Consequently, the zero-point energy in the parabolic approximation to the potential, but with the correct curvature, is to $O(n^{-1})$

$$\tfrac{1}{2}[U_n''((n\theta)^{1/2}) + \Delta U_n'']^{1/2} = \tfrac{1}{2}(\kappa_2^2 - 24\kappa/n\kappa_2^2)^{1/2}$$

$$\simeq \tfrac{1}{2}\kappa_2 - 6\kappa/n\kappa_2^3. \qquad (6.31)$$

Adding the combined classical and quantum contributions of Eq. (6.28) to the additional quantum contribution of Eq. (6.31) gives finally

$$E_n = E_\infty + E^{(1)}n^{-1} + E^{(2)}n^{-2} + \cdots, \qquad (6.32)$$

where the first and second terms are the Hartree expression, Eq. (3.7), and the correction, Eq. (5.12). The third term expresses the new higher-order correction

$$E^{(2)} = 12\frac{\kappa^2}{\kappa_2^4} - 6\frac{\kappa}{\kappa_2^3} + \frac{1}{4\kappa\kappa_2^4}. \qquad (6.33)$$

Asymptotic expressions for $E^{(2)}$ in the high- and low-temperature ranges are

$$E^{(2)} \simeq \begin{cases} -\tfrac{5}{64}\kappa^{-5} + \tfrac{23}{512}\kappa^{-8} \simeq -\tfrac{5}{64}\tau^{-5/2} + \tfrac{73}{512}\tau^{-8}, & \tau \gg 1 \\[2mm] \tfrac{1}{4}\kappa - 6\kappa^{5/2} \simeq \tfrac{1}{8}(\tau)^{-1} - (3/2^{3/2})(\tau)^{-5/2}, & \tau \ll -1. \end{cases}$$
$$(6.34)$$

Figure 12 shows a plot of Eq. (6.33), the second screening approximation, identified by the label "ss", as well as numerical computations of $n[n(E_n - E_\infty) - E^{(1)}]$ for $n = 1$, 2, 3, and 4. One sees that the main deviation of $n(E_n - E_\infty)$ from $E^{(1)}$, which was displayed in Fig. 7, has been accounted for by $E^{(2)}$. The residual deviation can be ascribed to the terms in Eq. (6.32) of $O(n^{-3})$ and higher. $E^{(3)}$ has been obtained numerically and is shown in Fig. 13 along with $E^{(1)}$ and $E^{(2)}$.

For the purpose of deriving second-screening-approximation formulas for the entropy and specific heat, it is convenient to reexpress Eq. (6.33) in terms of the correlation-length ratio $2\kappa/\kappa_2 = (1 + 2\theta^3)^{-1/2}$. Thus we find

$$E^{(2)} = 3\frac{1}{\kappa_2^2} - 6\frac{\kappa}{\kappa_2^3} - \frac{11}{4}\frac{1}{\kappa\kappa_2^4}$$

$$= \frac{3}{4\kappa^2}\left(\frac{2\kappa}{\kappa_2}\right)^2 - \frac{3}{4\kappa^2}\left(\frac{2\kappa}{\kappa_2}\right)^3 - \frac{11}{64\kappa^5}\left(\frac{2\kappa}{\kappa_2}\right)^4$$

$$= 3\theta^2(1 + 2\theta^3)^{-1} - 3\theta^2(1 + 2\theta^3)^{-3/2} - \tfrac{11}{2}\theta^5(1 + 2\theta^3)^{-2}$$

$$= \theta^2[\tfrac{1}{4}(1 + 2\theta^3)^{-1} - 3(1 + 2\theta^3)^{-3/2} + \tfrac{11}{4}(1 + 2\theta^3)^{-2}]. \qquad (6.35)$$

Substituting from Eq. (5.15), and denoting the quantity appearing within square brackets in Eq. (6.35) by $[\cdots]$, we find the second-screening-approximation fractional-entropy correction
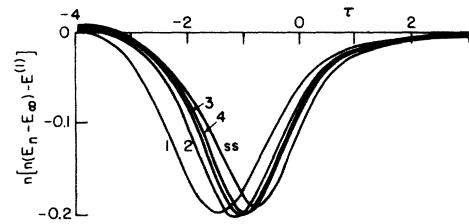

FIG. 12. Deviation of the free energy E_n from the first screening approximation $E_\infty + n^{-1}E^{(1)}$ vs reduced temperature τ. The cases $n = 1$, 2, 3, and 4 tend toward the second screening correction $E^{(2)}(\tau)$ (curve labeled "ss") in the limit $n \to \infty$.

$$\frac{\theta^{(2)}}{\theta} = \frac{2}{\theta}\frac{dE^{(2)}}{d\tau} = \frac{2}{\theta}\frac{d\theta}{d\tau}\frac{d}{d\theta}\,\theta^2\,[\cdots] = 2[-1+(1+2\theta^3)^{-1}]\left\{2[\cdots]+6\theta^3\frac{\partial[\cdots]}{\partial(1+2\theta^3)}\right\}$$

$$= 2[-1+(1+2\theta^3)^{-1}]\left\{2[\cdots]+3(1+2\theta^3)\frac{\partial[\cdots]}{\partial(1+2\theta^3)}-3\frac{\partial[\cdots]}{\partial(1+2\theta^3)}\right\}.$$ (6.36)

The first term of the first factor and the first and second terms within braces do not affect the power of $(1+2\theta^3)^{-1}$, while the second term of the first factor and the third term within braces increase the exponent by unity. Carrying out the indicated operations yields

$$\theta^{(2)}/\theta = \tfrac{1}{2}(1+2\theta^3)^{-1} - 15(1+2\theta^3)^{-3/2} + 20(1+2\theta^3)^{-2} + 42(1+2\theta^3)^{-5/2}$$

$$-\tfrac{107}{2}(1+2\theta^3)^{-3} - 27(1+2\theta^3)^{-7/2} + 33(1+2\theta^3)^{-4}.$$ (6.37)

Designating the right-hand side of Eq. (6.37) now by $[\cdots]$ and differentiating once more, we find for the second-order specific-heat correction

$$C^{(2)} = -\frac{d\theta^{(2)}}{d\tau} = -\frac{d\theta}{d\tau}\frac{d}{d\theta}\,\theta[\cdots] = [1-(1+2\theta^3)^{-1}]\left\{[\cdots]+3(1+2\theta^3)\frac{\partial[\cdots]}{\partial(1+2\theta^3)}-3\frac{\partial[\cdots]}{\partial(1+2\theta^3)}\right\}$$

$$= -(1+2\theta^3)^{-1}+\tfrac{105}{2}(1+2\theta^3)^{-3/2}-\tfrac{195}{2}(1+2\theta^3)^{-2}-393(1+2\theta^3)^{-5/2}+\tfrac{1283}{2}(1+2\theta^3)^{-3}+912(1+2\theta^3)^{-7/2}$$

$$-\tfrac{2785}{2}(1+2\theta^3)^{-4}-855(1+2\theta^3)^{-9/2}+\tfrac{2481}{2}(1+2\theta^3)^{-5}+\tfrac{567}{2}(1+2\theta^3)^{-11/2}-396(1+2\theta^3)^{-6}.$$ (6.38)

Figure 14 illustrates the application of Eq. (6.38) to the specific case $n=2$. The curve labeled "2" shows the exact numerical evaluation of $C_2(\tau)$ while "s" and "ss" show the first- and second-order approximations $C_\infty + C^{(1)}/2$ and $C_\infty + C^{(1)}/2 + C^{(2)}/4$, respectively. $[C^{(1)}(\tau)$ and $C^{(2)}(\tau)$ were computed from Eqs. (5.18) and (6.38), respectively.] It is evident that including the second-order term has modestly improved the accuracy of the approximation. It is interesting to note from Fig. 13 that $E^{(3)}$ is almost exactly proportional to the derivative of $E^{(2)}$. Thus the third-order correction will be equivalent simply to a shift of $E^{(2)}$ along the τ axis toward negative τ. Such a shift will very much better reproduce the true variation of C_2

with τ, as can be seen from the fact that the "s" curve crosses the "2" curve at τ values just 0.3 smaller than where it crosses the "ss" curve. It obviously would be worthwhile to carry the quantum-mechanical calculation to yet one higher order in n^{-1} in order to see if the resulting formula for $E^{(3)}$ is in fact reasonably represented by $\partial E^{(3)}/\partial\tau$. This, however, will remain a task for the future and we do not attempt it here.

VII. PERTURBATION THEORY AND SCREENING

In this section we present an abbreviated description of the application of the perturbation techniques of quantum field theory[17] to the prob-
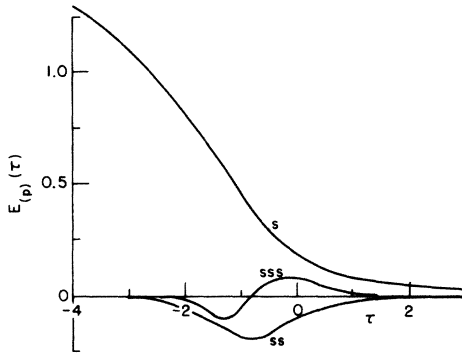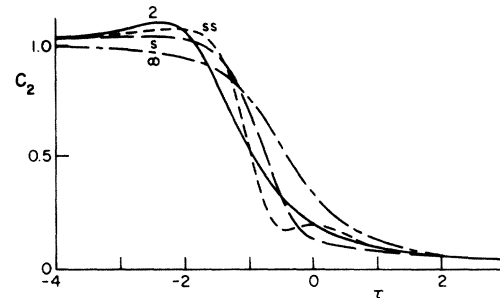
FIG. 13. Higher-order screening corrections $E^{(p)}(\tau)$ vs reduced temperature τ. The first-, second-, and third-order corrections for $p=1$, 2, and 3 are shown by the curves labeled "s," "ss," and "sss," respectively.

FIG. 14. Specific heat C_n vs reduced temperature τ for $n=2$. The curve labeled "2" shows the exact numerical results, while "∞" shows the Hartree approximation. The improvements upon the Hartree approximation are shown by the first and second screening approximations, which are plotted as the curves labeled "s" and "ss", respectively.

lem of the Ginzburg–Landau field in one dimen-
sion. We show how to establish contact with the
methods used previously in this paper and we
relate the results obtained earlier in this paper
to the method of screening which has been applied
to the general problem of the Ginzburg–Landau
field in an arbitrary number of dimensions (e.g.,
$D = 3$ and $D = 2$).[18] First we note that the problem
posed by Eqs. (1.8), (1.10), and (1.11) is trivially
solvable in the absence of the fourth-order an-
harmonic term in the Lagrangian L_n. It is, there-
fore, natural to attempt a perturbation expansion
in the anharmonic term, which we distinguish by
a prime,

$$L_n'(u) = -(4n)^{-1} \sum_{i,j} \phi_i^2(u)\phi_j^2(u) . \tag{7.1}$$

According to Eq. (1.8) we have to expand the ex-
ponential function $\exp \int L_n'(u)\,du$. The individual
terms in this expansion are to be summed over
all configurations of the n-component ϕ field.
According to Eq. (1.15) such sums, or functional
integrals, can be written as averages carried out
over the noninteracting field, which we denote
by the subscript 0. This gives for the ratio of
the additional portion of the partition function to
the unperturbed partition function,

$$\frac{\Delta Z_0^{(n)}}{Z_{\Omega 0}^{(n)}} = \frac{Z_\Omega^{(n)}}{Z_{\Omega 0}^{(n)}} - 1$$

$$= \int d1\langle L_n'(1)\rangle_0 + \frac{1}{2!}\int\int d1\,d2\langle L_n'(1)L_n'(2)\rangle_0$$

$$+ \frac{1}{3!}\int\int\int d1\,d2\,d3\langle L_n'(1)L_n'(2)L_n'(3)\rangle_0 + \cdots . \tag{7.2}$$

As already stated, the subscript on the angular
brackets indicates that these averages are to be
computed according to Eq. (1.15) by dropping L_n'
from L_n. The coordinates u_1, u_2, and u_3 of vari-
ous points are abbreviated by 1, 2, and 3, re-
spectively. The zero-order free-energy density
in the absence of interaction is given according
to Eq. (1.11) by

$$\mathcal{F}_{n0} = -(1/n\Omega)\ln Z_{\Omega 0}^{(n)} \tag{7.3}$$

and is found in Eqs. (2.6) and (2.7) to be, up to an
additive constant, $\tau^{1/2}/2$. By expanding the loga-
rithm we find for the remaining portion of the
free-energy density

$$\Delta\mathcal{F}_n = \mathcal{F}_n - \mathcal{F}_{n0} = -\frac{1}{n\Omega}\ln\left[1 + \frac{\Delta Z_\Omega^{(n)}}{Z_{\Omega 0}^{(n)}}\right]$$

$$= -\frac{1}{n\Omega}\frac{\Delta Z_\Omega^{(n)}}{Z_{\Omega 0}^{(n)}} + \frac{1}{2n\Omega}\left[\frac{\Delta Z_\Omega^{(n)}}{Z_{\Omega 0}^{(n)}}\right]^2 - \frac{1}{3n\Omega}\left[\frac{\Delta Z_\Omega^{(n)}}{Z_{\Omega 0}^{(n)}}\right]^3 + \cdots . \tag{7.4}$$

By substituting from Eq. (7.2) and regrouping
the terms according to the number of times L_n'
occurs, we obtain the perturbation expansion

$$\Delta\mathcal{F}_n = \mathcal{F}_{n1} + \mathcal{F}_{n2} + \mathcal{F}_{n3} + \cdots , \tag{7.5}$$

where the first-order term is simply

$$\mathcal{F}_{n1} = -\frac{1}{n\Omega}\int d1\langle L_n'(1)\rangle_0 = -\frac{1}{n}\langle L_n'\rangle_0 . \tag{7.6}$$

The second-order term $\mathcal{F}_{n2}$ receives contributions
from both the first and second terms of Eq. (7.4).
These two terms tend to cancel one another so as
to leave the result independent of the volume Ω
of the system. The result depends only on the
correlation function for L_n' according to

$$\mathcal{F}_{n2} = -\frac{1}{2n\Omega}\int\int d1\,d2[\langle L_n'(1)L_n'(2)\rangle_0$$

$$-\langle L_n'(1)\rangle_0\langle L_n'(2)\rangle_0]$$

$$= -\frac{1}{2n\Omega}\int\int d1\,d2\langle \delta L_n'(1)\,\delta L_n'(2)\rangle_0$$

$$= -\frac{1}{2n}\int d12\langle \delta L_n'(1)\,\delta L_n'(2)\rangle_0 . \tag{7.7}$$

Ω cancels out in the last line because in a homo-
geneous system the correlation function depends
only upon the relative coordinate $12 \equiv u_1 - u_2$. Here
the subtraction which occurs leads to the correla-
tion of the fluctuations of the perturbed term of
the Lagrangian,

$$\delta L_n'(u) \equiv L_n'(u) - \langle L_n\rangle_0 . \tag{7.8}$$

This cancellation of the unphysical terms in the
free-energy density (i.e., those which would de-
pend on the volume linearly or on higher powers
of the volume) is, of course, essential for a phys-
ically acceptable perturbation expansion, and is
familiar in the many-body problem and in quantum
field theory as the linked-cluster expansion. Only
linked clusters contribute to the free energy in
a statistical-mechanics problem or to the ground-
state energy of a many-body quantum system. The
unlinked clusters which occur in $Z_\Omega^{(n)}$ and which
depend on higher powers of Ω cancel out of the
perturbation expansion for $\mathcal{F}_n$. In this section we
exhibit in detail only the calculations through
second order of perturbation theory and for the
sake of brevity shall simply sketch schematically
the contributions of higher order. A detailed
treatment of the application of higher-order per-
turbation theory to the one-dimensional Ginzburg–
Landau field will be postponed to a later publica-
tion.[19]

We now proceed to evaluate the first- and
second-order contributions, Eqs. (7.6) and (7.7).

In this it is necessary to treat the terms in the sum in Eq. (7.1) differently depending upon whether the indices i and j are unequal or equal. When $i \neq j$ the expectation value factors because of the statistical independence of the fluctuations of the ith and jth field components in zero order:

$$\langle \phi_i^2 \phi_j^2 \rangle_0 = \langle \phi_i^2 \rangle_0 \langle \phi_j^2 \rangle_0 = G_0^2(0) . \qquad (7.9)$$

$G_0(0)$ is the order-parameter correlation function evaluated at zero separation, and will be computed further below. First we pass on to the case $i = j$, where there are now three ways in which the field variables can be paired, giving the factorization

$$\langle \phi_i^4 \rangle_0 = 3 \langle \phi_i^2 \rangle_0 \langle \phi_i^2 \rangle_0 = 3 G_0^2(0) . \qquad (7.10)$$

Therefore, in summing j over all n values, we have to add a correction term of $+2$ for the case $j = i$. The result of the summation is thus an overall factor of $n + 2$. The remaining sum over i yields an additional factor of n, so substituting Eqs. (7.1), (7.9), and (7.10) into Eq. (7.6) gives

$$\mathcal{F}_{n1} = \frac{1}{4n^2} \sum_{i,j} \langle \phi_i^2 \phi_j^2 \rangle$$

$$= \frac{1}{4n^2} n(n+2) G_0^2(0) = \frac{1}{4} G_0^2(0) + \frac{1}{2n} G_0^2(0) . \qquad (7.11)$$

The correlation function is the Fourier integral

$$G_0(12) = \langle \phi_i(1)\phi_i(2) \rangle$$

$$= \frac{1}{2\pi} \int dp\, g_0(p, \kappa_0) e^{ipu_{12}} , \qquad (7.12)$$

where the Fourier component is

$$g_0(p, \kappa_0) = 1/(p^2 + \kappa_0^2) \qquad (7.13)$$

and κ_0 is the inverse correlation length in the absence of interaction, as discussed in connection with Eqs. (3.4) and (3.5). Carrying out the Fourier integral gives explicitly

$$G_0(12) = (1/2\kappa_0) e^{-\kappa_0 |u_{12}|} , \qquad (7.14)$$

so that at zero separation we obtain

$$G_0(0) = 1/2\kappa_0 . \qquad (7.15)$$

Substitution of Eq. (7.15) into Eq. (7.11) gives the first-order correction

$$\mathcal{F}_{n1} = 1/16\kappa_0^2 + 1/8n\kappa_0^2 . \qquad (7.16)$$

We note that the first term in Eq. (7.16) is identical to the leading correction to the free energy found in Eq. (3.9). The second term in Eq. (7.16) of $O(n^{-1})$ is identical to the leading term in Eq. (5.12).
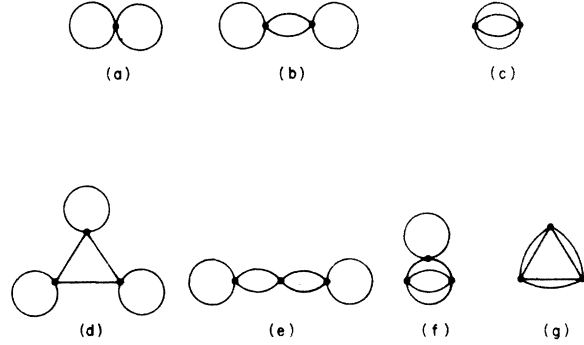

FIG. 15. Feynman diagrams for the free energy showing the first-order contribution (a), the second-order (b) and (c), and all third-order diagrams (d)−(g).

The higher-order terms in the perturbation expansion are the more complicated to evaluate and it is useful to depict the integrals encountered by means of the Feynman diagrams of Fig. 15. Graph (a) illustrates the first-order calculation just completed, while (b) and (c) correspond to the integrals required for $\mathcal{F}_{n2}$. We designate these parts by $\mathcal{F}_{n2b}$ and $\mathcal{F}_{n2c}$, respectively. If we denote the indices at 1 by i and j and those at 2 by i' and j', then we see that graph (b) requires one of the indices i' or j' to equal either i or j, assuming $i \neq j$. This gives factors of 2 at both points. If we denote the remaining index at 2 as $k \neq j$, then the sum over all such cases contributes to the required correlation function the amount

$$\sum_j \sum_{\substack{i \neq j \\ k \neq j}} 4 \langle \delta[\phi_i^2(1)\phi_j^2(1)] \delta[\phi_j^2(2)\phi_k^2(2)] \rangle_{0b}$$

$$= 4(n-1)^2 \langle \phi_i^2 \rangle_0 \langle \phi_k^2 \rangle_0 \sum_j \langle \delta \phi_j^2(1) \delta \phi_j^2(2) \rangle_0$$

$$= 4n(n-1)^2 G_0^2(0) \langle \delta \phi_j^2(1) \delta \phi_j^2(2) \rangle_0 . \qquad (7.17)$$

The subscript b in the above average excludes the additional term which arises from $k = i$. This term corresponds to graph (c) and will be computed further below. But we must include with graph (b) those cases when $k = j$ or $i = j$. In the latter case we lose the factor of 2 associated with the choice of which index at point 1 to pair with point 2, but we replace this factor with the combinatorial factor $4 \times 3 / 1 \times 2 = 6$ representing the number of ways in which two factors of $\phi_j(1)$ can be chosen out of $\phi_j^4(1)$; i.e.,

$$\langle \delta \phi_j^4(1) \delta[\phi_j^2(2)\phi_k^2(2)] \rangle_{0b} = \langle \delta \phi_j^4(1) \delta \phi_j^2(2) \rangle_0 \langle \phi_k^2 \rangle_0$$

$$= 6 \langle \phi_j^2 \rangle_0 \langle \phi_k^2 \rangle_0 \langle \delta \phi_j^2(1) \delta \phi_j^2(2) \rangle_0 ,$$

$$(7.18)$$

and similarly for $k = j$. (The special case $k = i = j$ is handled in the same way.) Thus we see that the factor $(n - 1)^2$ in Eq. (7.17) has to be replaced by $(n + 2)^2$, giving for the required correlation function

$$\langle \delta L_n'(1) \delta L_n'(2) \rangle_{ob} = \frac{(n + 2)^2}{4n} G_0^2(0) \langle \delta \phi_j^2(1) \delta \phi_j^2(2) \rangle_0 .$$

$$(7.19)$$

The last factor in this equation can be evaluated by pairing the field variables in two different ways to yield

$$\langle \delta \phi_j^2(1) \delta \phi_j^2(2) \rangle_0 = 2G_0^2(12) .$$

$$(7.20)$$

It is convenient to write $G_0^2(12)$ as the Fourier integral

$$G_0^2(12) = \frac{1}{2\pi} \int dq \, \Pi_0(q, \kappa_0) e^{iqu_{12}} .$$

$$(7.21)$$

As $G_0^2(12) = k_0^{-1}(4k_0)^{-1} e^{-2k_0(u_{12})}$ is of the same form as $G_0(12)$ itself, it follows in analogy with Eq. (7.13) that

$$\Pi_0(q, \kappa_0) = \kappa_0^{-1}/(q_0^2 + 4\kappa_0^2) .$$

$$(7.22)$$

Substitution of Eqs. (7.22) and (7.19) into Eq. (7.7) gives

$$\mathcal{F}_{n2b} = -\frac{1}{4}\left(1 + \frac{2}{n}\right)^2 G_0^2(0) \int d12 \, G_0^2(12)$$

$$= -\left(\frac{1}{4} + \frac{1}{n} + \frac{1}{n^2}\right)\frac{1}{4\kappa_0^2} \Pi_0(o, \kappa_0)$$

$$= -\frac{1}{64\kappa_0^5} - \frac{1}{16n\kappa_0^5} - \frac{1}{16n^2\kappa_0^5} .$$

$$(7.23)$$

Turning now to graph (c), we have two different ways in which the indices i' and j' at 2 can match i and j at 1. Thus the sum over j for $j \neq i$ is

$$\sum_{j \neq i} 2 \langle \delta[\phi_i^2(1)\phi_j^2(1)] \delta[\phi_i^2(2)\phi_j^2(2)] \rangle_{oc}$$

$$= 2 \sum_{j \neq i} \langle \delta \phi_i^2(1) \delta \phi_i^2(2) \rangle_0 \langle \delta \phi_j^2(1) \delta \phi_j^2(2) \rangle_0$$

$$= 8(n - 1)G_0^4(12) .$$

$$(7.24)$$

On the other hand, when $j = i$ the pairing between points 1 and 2 can be accomplished in $4! = 24 = 3 \times 8$ different ways. Consequently, as before, the factor $n - 1$ in Eq. (7.24) has to be replaced by $n + 2$, giving for the required correlation function

$$\langle \delta L_n'(1) \delta L_n'(2) \rangle_{oc} = \frac{n + 2}{2n} G_0^4(12) .$$

$$(7.25)$$

Substituting this result into Eq. (7.7) gives the corresponding contribution to the free energy,

$$\mathcal{F}_{n2c} = -\frac{n + 2}{4n^2} \int d12 \, G_0^4(12)$$

$$= -\frac{1}{64\kappa_0^4}\left(\frac{1}{n} + \frac{2}{n^2}\right) \int_{-\infty}^{+\infty} du_{12} \, e^{-4\kappa_0|u_{12}|}$$

$$= -\frac{1}{128n\kappa_0^5} - \frac{1}{64n^2\kappa_0^5} .$$

$$(7.26)$$

The sum of Eqs. (7.26) and (7.23) gives the total second-order correction

$$\mathcal{F}_{n2} = \mathcal{F}_{n2b} + \mathcal{F}_{n2c}$$

$$= -\frac{1}{64\kappa_0^5} - \frac{9}{128n\kappa_0^5} - \frac{5}{64n^2\kappa_0^5} .$$

$$(7.27)$$

These terms are identical to the third term in Eq. (3.9), the second term in Eq. (5.12), and the first term in Eq. (6.34), respectively.

Let us denote the term in $\mathcal{F}_{n\nu}$ of order $n^{-\mu}$ by $\mathcal{F}_\nu^{(\mu)}$ and collect all of the $\mu = 0$, or "Hartree," terms to obtain, from Eqs. (7.16) and (7.27),

$$\mathcal{F}_\infty = \frac{1}{2}\kappa_0 + \mathcal{F}_1^{(0)} + \mathcal{F}_2^{(0)} + \cdots$$

$$= \frac{1}{2}\kappa_0 + \frac{1}{16\kappa_0^2} - \frac{1}{64\kappa_0^5} + \cdots ,$$

$$(7.28)$$

in agreement with Eq. (3.9). Similarly, the $\mu = 1$ terms combine to give

$$\mathcal{F}^{(1)} = \mathcal{F}_1^{(1)} + \mathcal{F}_{2b}^{(1)} + \mathcal{F}_{2c}^{(1)} + \cdots$$

$$= \frac{1}{8\kappa_0^2} - \frac{1}{16\kappa_0^5} - \frac{1}{128\kappa_0^5} + \cdots$$

$$= \frac{1}{8\kappa^2} - \frac{1}{128\kappa^5} + \cdots .$$

$$(7.29)$$

Here we have used Eq. (3.5a) to introduce κ, the Hartree self-consistent reciprocal correlation length. This corresponds to "dressing" the $i = j$ parts of graph (a) of Fig. 15 by the closed-loop appendage shown in (b). Further such dressing in third-order perturbation theory is illustrated by graphs (d) and (e). Thus, the problem is greatly simplified and many of the graphs shown in Fig. 15 are automatically included if we use dressed lines, which by definition include all possible closed-loop appendages. This corresponds to a rearrangement and partial summation of the perturbation expansion. If we denote by a bar the terms in perturbation theory evaluated in such a way, we have in "first order" (containing in fact all higher-order dressings)

$$\bar{\mathcal{F}}_1^{(1)} = \frac{1}{8\kappa^2} = \frac{1}{2} G^2(0) = \frac{1}{4\pi} \int dq \Pi_0(q, \kappa) .$$

$$(7.30)$$

In this rearrangement of terms, graph (b) is in-

cluded in $\mathcal{F}_1^{(1)}$ and no longer needs to be considered explicitly. The only second-order graph not automatically included by dressing graph (a) is (c), which in turn gets dressed in third order by graph (f). The latter is therefore included implicitly in

$$\mathcal{F}_{2c}^{(1)} = -\frac{1}{128\kappa^5} = -\frac{1}{4}\int d12\, G^4(12)$$

$$= -\frac{1}{8\pi}\int dq\, \Pi_0^2\,(q,\kappa)\,. \tag{7.31}$$

The second line follows from dropping the subscript zero from $G_0(12)$ in Eq. (7.26)—indicating that κ is to be used instead of κ_0. Substituting from Eq. (7.21) gives the last line.

As already stated, graph (f) of Fig. 15 is included in Eq. (7.31) as a dressing of (c). Similarly, graphs (e) and (d) are included in Eq. (7.30) as higher-order dressings of (a). These three graphs are the third-order perturbation diagrams describing one, two, and three closed-loop dressings, respectively. The only third-order graph not yet included is (g), containing no appendages. Including higher-order dressings, we find

$$\mathcal{F}_{3h}^{(1)} = \frac{1}{12\pi}\int dq\Pi_0^3(q,\kappa)\,. \tag{7.32}$$

Equations (7.30), (7.31), and (7.32) can be combined to give

$$\mathcal{F}^{(1)} = \mathcal{F}^{(1)} = \mathcal{F}_1^{(1)} + \mathcal{F}_{2c}^{(1)} + \mathcal{F}_{3h}^{(1)} + \cdots$$

$$= \frac{1}{4\pi}\int dq\,(\Pi_0 - \tfrac{1}{2}\Pi_0^2 + \tfrac{1}{3}\Pi_0^3 - \cdots)$$

$$= \frac{1}{4\pi}\int dq\,\ln(1+\Pi_0)\,. \tag{7.33}$$

Equation (7.33) is the special case $D = 1$ of the general first-order screening formula[20]

$$\delta\mathcal{F} = \frac{1}{2(2\pi)^D}\int d^Dq\,\ln[1+\Pi_0(q,\kappa)] \tag{7.34}$$

and can be readily evaluated by integrating by parts:

$$\mathcal{F}^{(1)} = \frac{1}{\pi\kappa}\int_0^\infty \frac{q^2\,dq}{(q^2+\kappa_2^2)\,(q^2+4\kappa^2)}$$

$$= \frac{\kappa_2^2}{\pi}\int_0^\infty \frac{dq}{q^2+\kappa_2^2} - \frac{4\kappa^2}{\pi}\int_0^\infty \frac{dq}{q^2+4\kappa^2}$$

$$= \frac{1}{2}(\kappa_2 - 2\kappa)\,. \tag{7.35}$$

Eq. (7.35) is identical to $E^{(1)}$ of Eq. (5.11), the $O(n^{-1})$ correction to the energy obtained by the method of quantum-mechanical equivalence.
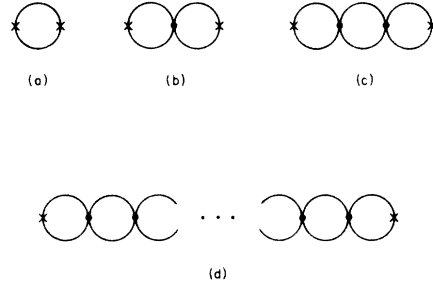

FIG. 16. Feynman diagrams for the pair propagator. (a) shows the bare propagator $\pi_0(q,\kappa)$, while (b) and (c) illustrate first- and second-order corrections, respectively. The sum of all the open-chain diagrams of type (d) gives the screened propagator $\pi(q,\kappa)$.

To conclude this section, we give a brief discussion of the power series in Π_0 which is contained in the integrand of Eq. (7.33). The ring diagrams shown in graphs (a), (c), and (g) of Fig. 15, if opened up into open chains, become graphs (a), (b), and (c), respectively, of Fig. 16. Summing to all orders of perturbation theory, corresponding to graph (d), gives the "screened" pair propagator

$$\Pi(q,\kappa) = \Pi_0 - \Pi_0^2 + \Pi_0^3 - \cdots$$

$$= \frac{\Pi_0}{1+\Pi_0} = \frac{1}{1+\Pi_0^{-1}}$$

$$= \frac{1}{1+\kappa q^2 + 4\kappa^3} = \frac{\kappa^{-1}}{q^2 + \kappa_2^2}\,, \tag{7.36}$$
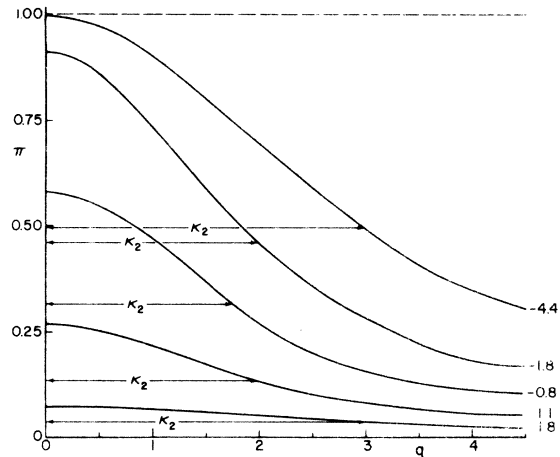

FIG. 17. Screened pair propagator $\pi(q,\kappa)$ vs q for different values of τ (labeled at the ends of the curves). The inverse of the wave vector κ_2 sets the range of the spatial correlations of the square of the order parameter. As τ decreases from 1.8 to -4.4, κ_2 decreases to a minimum at $\tau = -0.75$ and then increases.

where the new reciprocal correlation length

$$\kappa_2 = (4\kappa^2 + \kappa^{-1})^{1/2} \qquad (7.37)$$

has already been encountered in Eq. (3.15) and is plotted as a function of τ in Fig. 5. Substituting from Eq. (3.16), we see that the screened pair propagator can alternatively be written as

$$\Pi(q, \kappa) = \frac{C_\infty(\tau)}{1 + q^2/\kappa_2^2}. \qquad (7.38)$$

Equation (7.38) is plotted in Fig. 17 for five different values of τ. It will be noted that $\Pi(q, \kappa)$ at first becomes more peaked as τ decreases, corresponding to decreasing κ_2. But as τ becomes negative, the Hartree specific heat $C_\infty(\tau)$ begins to saturate at unity, its $\tau \to -\infty$ asymptotic value, and the plot of $\Pi(q, \kappa)$ becomes flatter again—corresponding to the rise in κ_2 shown in Fig. 5, to the left of the minimum.

VIII. SUMMARY

We have studied the classical statistical mechanics of an n-dimensional order parameter which exists in one spatial dimension. This many-body (field) problem was reduced to a quantum-mechanical one-body problem which we solved numerically. It, therefore, provides a convenient testing ground for studying the convergence as well as understanding the nature of approximations used for higher spatial dimensions. Here we have shown in various figures how the results for finite n converge toward the $n = \infty$ answer. In addition, we have investigated the n^{-1} expansion by computing the first- and second-order corrections to the $n = \infty$ result.

We find that the second screening approximation improves the accuracy in a kind of mean-square sense. This can be seen directly in Fig. 14, where we have plotted the exact specific heat for $n = 2$ and the zeroth (Hartree), first, and second screening approximations given by C_∞, $C_\infty + \frac{1}{2}C^{(1)}$, and $C_\infty + \frac{1}{2}C^{(1)} + \frac{1}{4}C^{(2)}$, respectively. Note the oscillatory fit of the second screening approximation $(C_\infty + \frac{1}{2}C^{(1)} + \frac{1}{4}C^{(2)})$ to C_2. Computing $C^{(3)}$ would clearly be worthwhile.

The nature of the large-n limit was discussed in terms of a stochastic peaking which takes place in the distribution function of ϕ when $n \to \infty$. It is this effect which allows one to obtain results for all temperatures (and spatial dimensions) when $n \gg 1$.

The quantum-mechanical formulation of the problem provides insight into the n^{-1} expansion. This was previously developed for higher spatial dimensions as a selective summation of certain Feynman graphs. In the quantum problem, the n dependence of the kinetic energy was eliminated in favor of adding a centrifugal term to the potential. Then the screening approximation was seen to arise simply from expanding this new potential about its minimum. Keeping the value of the potential at its minimum to order n^{-1} and adding the zero-point motion about the minimum with the curvature calculated to order n^0 gave the first screening approximation. Expanding both of these effects out one more order in n and including in lowest order the anharmonic part of the potential leads to the second screening approximation. It will be interesting to study the Feynman graphs which give rise to the second-order screening approximation since we now know their contribution for the case of one spatial dimension.[19,21]

*Research supported in part by the Office of Naval Research.

†Work supported by the National Science Foundation.

[1]L. Onsager, Phys. Rev. 65, 117 (1944).

[2]This is no longer true for the extension of the problem to values of $n < 1$. R. Balian and G. Toulouse, Phys. Rev. Lett. 30, 544 (1973); Ann. Phys. (N.Y.) (to be published).

[3]M. E. Fisher, Phys. Rev. Lett. 30, 679 (1973).

[4]R. J. Londergan and J. S. Langer, Phys. Rev. B 5, 4376 (1972).

[5]L. W. Gruenberg and L. Gunther, Phys. Lett. A 38, 463 (1972).

[6]D. J. Scalapino, M. Sears, and R. A. Ferrell, Phys. Rev. B 6, 3409 (1972).

[7]S. Grossman, P. H. Richter, and C. Wissel, Solid State Commun. 11, 433 (1972).

[8]A. J. Bray and G. Rickayzen, J. Phys. F 2, L109 (1972);

R. A. Ferrell and D. J. Scalapino, Phys. Rev. Lett. 29, 413 (1972); Phys. Lett. A 41, 37 (1972).

[9]R. Abe, Prog. Theor. Phys. 48, 1414 (1972); S. K. Ma, Phys. Rev. Lett. 29, 1311 (1972).

[10]R. P. Feynman and A. R. Hibbs, Quantum Mechanics and Path Integrals (McGraw-Hill, New York, 1965).

[11]V. L. Ginzburg and L. D. Landau, Zh. Eksp. Teor. Fiz. 20, 1064 (1950).

[12]R. A. Ferrell, J. Low Temp. Phys. 1, 241 (1969).

[13]L. Gunther and L. W. Gruenberg, Solid State Commun. 10, 567 (1972).

[14]See Ref. 6, for example.

[15]Extensive Rayleigh-Schrödinger perturbation results obtained by expanding in b have been given for the one-dimensional anharmonic oscillator by C. M. Bender and T. T. Wu, Phys. Rev. Lett. 27, 461 (1971); Phys. Rev. D 7, 1620 (1973).

[16]R. A. Ferrell, Phys. Rev. Lett. 1, 518 (1958).

[17]Quantum-field-theory techniques are discussed in Refs. 8 and 9. In addition, see A. J. Bray, Ph.D. thesis (University of Kent, 1973) (unpublished); Screening Solution in Zero- and One-Dimensional Ginzburg-Landau Systems, University of Kent report (1972) (unpublished).

[18]The first screening approximation has recently been carried out for $D = 2$ by D. J. Scalapino, R. A. Ferrell and A. J. Bray, Phys. Rev. Lett. 31, 292 (1973).

[19]A. J. Bray, University of Maryland Department of Physics and Astronomy Technical Report No. 74-049 (1973) (unpublished).

[20]R. A. Ferrell and D. J. Scalapino, Phys. Lett. A 41, 37 (1972).

[21]Bray has recently demonstrated how the zero-dimensional problem also provides a useful check on the graphical expansion [A. J. Bray, University of Maryland Department of Physics and Astronomy Technical Report No. 74-045 (1973) (unpublished)].